AFRL-RH-BR-TR-2009-0051

Modeling Mesopic Vision Based on Measured Photoreceptor Sensitivity

Jim Dykes
University of Texas at San Antonio
One UTSA Circle
San Antonio, TX 78249-1644

July 2009
Final Report for June 2007-January 2009

Air Force Research Laboratory
Human Effectiveness Directorate
Directed Energy Bioeffects Division
Optical Radiation Branch
Brooks City-Base, TX 78235

NOTICE AND SIGNATURE PAGE

Using Government drawings, specifications, or other data included in this document for any purpose other than Government procurement does not in any way obligate the U.S. Government. he fact that the Government formulated or supplied the drawings, specifications, or other data does not license the holder or any other person or corporation; or convey any rights or permission to manufacture, use, or sell any patented invention that may relate to them.

This report was cleared for public release by the 311th Public Affairs Office at Brooks City Base, TX and is available to the general public, including foreign nationals. Copies may be obtained from the Defense Technical Information Center (DTIC) (http://www.dtic.mil).

AFRL-RH-BR-TR-2009-0051 HAS BEEN REVIEWED AND IS APPROVED FOR PUBLICATION IN ACCORDANCE WITH ASSIGNED DISTRIBUTION STATEMENT.

__//SIGNED//_____
Leon N. McLin, Jr., O.D., M.S.
Contract Representative

__//SIGNED// _____
GARRETT D. POLHAMUS, Ph.D.
Chief, Directed Energy Bioeffects Division
Human Effectiveness Directorate
711 Human Performance Wing
Air Force Research Laboratory

This report is published in the interest of scientific and technical information exchange, and its publication does not constitute the Government's approval or disapproval of its ideas or findings.

REPORT DOCUMENTATION PAGE

Form Approved
OMB No. 0704-0188

1. REPORT DATE *(DD-MM-YYYY)*	2. REPORT TYPE	3. DATES COVERED *(From - To)*
July 2009	Final Technical Report	Jun 2007 – Jan 2009

4. TITLE AND SUBTITLE

Modeling Mesopic Vision Based on Measured Photoreceptor Sensitivity

5a. CONTRACT NUMBER

5b. GRANT NUMBER
FA8650-07-1-6849-UTSA

5c. PROGRAM ELEMENT NUMBER
0602202F

6. AUTHOR(S)

Jim Dykes

5d. PROJECT NUMBER
7757

5e. TASK NUMBER
B2

5f. WORK UNIT NUMBER
34

7. PERFORMING ORGANIZATION NAME(S) AND ADDRESS(ES)
The University of Texas at San Antonio
One UTSA Circle
San Antonio, TX 78249-1644

8. PERFORMING ORGANIZATION REPORT NUMBER

9. SPONSORING / MONITORING AGENCY NAME(S) AND ADDRESS(ES)

Air Force Materiel Command
Air Force Research Laboratory
Human Effectiveness Directorate
Directed Energy Bioeffects Division
Optical Radiation Branch
2624 Louis Bauer Dr.
Brooks City-Base, TX 78235-5128

10. SPONSOR/MONITOR'S ACRONYM(S)
AFRL 711 HPW/ RHDO

11. SPONSOR/MONITOR'S REPORT NUMBER(S)
AFRL-RH-BR-TR-2009-0051

12. DISTRIBUTION / AVAILABILITY STATEMENT
Approved for public release; distribution is unlimited.

13. SUPPLEMENTARY NOTES
Contract Representative – Leon N. McLin, Jr., O.D., M.S.

14. ABSTRACT

A series of seven experiments were conducted under the HBCU/MI grant from AFRL/RHDO to study brightness, contrast acuity, contrast sensitivity, and color appearance across the mesopic range (between full photopic and full scotopic vision). The transition from cone to rod inputs was measured for each dependent variable and the relative contributions of the l-, m-, and s-cones were measured for each dependent variable across the mesopic range. The data consistently show the decrease in importance of the l-cones and the critical importance of s-cones in the mesopic range. These data can inform decisions about aircrew safety in mesopic conditions and specific suggestions are offered for color appearance modeling.

15. SUBJECT TERMS
Mesopic vision, contrast acuity, contrast sensitivity, color appearance,

16. SECURITY CLASSIFICATION OF:			17. LIMITATION OF ABSTRACT	18. NUMBER OF PAGES	19a. NAME OF RESPONSIBLE PERSON
					Leon N. McLin, Jr.
a. REPORT	b. ABSTRACT	c. THIS PAGE			19b. TELEPHONE NUMBER *(include area code)*
Unclassified	Unclassified	Unclassified	SAR	63	

Standard Form 298 (Rev. 8-98) **Prescribed by ANSI Std. Z39.18**

This page intentionally left blank

TABLE OF CONTENTS

LIST OF FIGURES

LIST OF TABLES

1. INTRODUCTION

Classic vision science research has focused on photopic vision (above about 10cd/m²) and scotopic vision (below about 10^{-2} cd/m²). Their respective luminosity functions are well established cornerstones of vision science and have been iteratively refined and parameterized. The basis of photopic vision on the l-, m-, and s-cones and the basis of scotopic vision on rods are noted in every introductory psychology textbook. A discussion of our physiological knowledge of bipolar cells and the magnocellular and parvocellular pathways is included in undergraduate sensation and perception textbooks as well as discussions of the luminance and color-opponent channels.

On the other hand, research into mesopic vision (the transition range between photopic and scotopic vision), is a relatively new research area and has yet to make it into undergraduate textbooks. Despite its lack of recognition due to currency, mesopic research is critical both theoretically and operationally. The theoretical research has focused on the relative contributions and interactions between the cones and rods in the mesopic range and on the implications for our visual processing channels. For instance, an early model of color appearance proposed by Hunt[1] included rod adaptation in mesopic vision. Rod adaptation was subsequently included in the CIECAM97s model[2]. More recent research has corroborated its importance[3,4]. Other research has focused on the uniqueness of the blue- yellow channel[5] and the finding that rod input may be interpreted as M-cone input within the chromatic channels[6]. TC 1-58 (Visual Performance in the Mesopic Range) was established in 2000 and the European Union's contribution to TC 1-58 (the Mesopic Optimization of Visual Efficiency Project[7]) proposed weights for the scotopic efficiency function in the mesopic range.

Mesopic vision is just as important operationally as it is theoretically. The Department of Transportation has focused on the high rates of accidents at dusk as a factor of drowsiness and complex secondary tasks[8]. Much of the AFRL mission is predicated on the principle that "We own the night". Baldwin et al.[9] made it clear that the ambient level of night time USAF missions is mesopic. It is mission critical to understand and predict the visual acuity and color appearance of an aircrew member looking under or around a NVG at cockpit displays and at an out-of-cockpit environment under less than or equal to moonlight ambient levels.

This research combined a theoretical focus on photoreceptor inputs with a focus on aircrew performance. The seven experiments were designed to measure brightness, contrast acuity, contrast sensitivity, and color appearance for both CRT displays and broad-band stimuli from low photopic through mesopic and into scotopic ambient levels. These results complement and extend research conducted by the AFRL711 HPW/ RHDO psychophysics lab. It should be noted that the experiment numbering in this final report is based on the experiment numbering used in the HBCU/MI proposal for consistency. The numbering sequence does not relate to the order in which the experiments were conducted. Neither does it relate to their order discussed in this final report (chosen to facilitate ease of reporting the results).

2. EXP 1: HETEROCHROMATIC FLICKER PHOTOMETRY & MINIMALLY DISTINCT BORDER

2.1 Rationale

The CIE 2-degree photopic luminosity function[10] and the scotopic luminosity function[11] are well established and available at http://cvision.ucsd.edu. Sharpe et al. (2005)[12] estimated that the photopic function is a linear combination of the l–cone and the m-cone sensitivities with weights of 0.690 and 0.348, respectively. Scotopic vision is based on rods. Experiment 1 investigated the relative contributions of the l-cones, m-cones, s-cones, and rods across the mesopic range using two different tasks: heterochromatic flicker photometry (HFP) and minimally distinct border (MDB).

2.2 Method

2.2.1 Participants

All participants were recruited from PSY 1013 (Introductory Psychology) in partial fulfillment of a course requirement. They had to self-report normal uncorrected acuity, normal color vision, and a minimum of 18 years of age in the on-line sign-up system. After arriving at the lab, each participant was screened using a high contrast Bailey Lovie chart and the Dvorine pseudoisochromatic plates. Of the first 12 students recruited for Experiment 1, three produced results that exceeded a 5 sem criterion for over 20% of the trials. They were replaced by three additional participants. The final set of 12 participants included seven males and five females with a mean age of 19.4 years (18- 23).

2.2.2 Design and Stimuli

The experiment was a 5 test conditions (4 HFP sizes and 1 MDB size) X 4 chromatic stimuli (red, green, blue & red, and blue & green) X 8 luminance levels (18.3, 4.6, 1.2, 0.29, 0.07, 0.02, 0.005, 0.001 cd/m^2) repeated measures design. All stimuli were presented on a Sony GDM-C520 CRT viewed from a distance of 46.5 inches. The HFP stimuli were squares of four sizes: 1, 2, 4, and 8 degrees of visual angle. The MDB stimuli consisted of two horizontally aligned rectangles (each 2 degrees wide and 4 degrees high; a 4 x 4 degree square together). In the HFP task, a neutral, achromatic square was flickered with a chromatic square on each trial. In the MDB task, the neutral, achromatic rectangle was to the right of the chromatic rectangle on each trial. Kaiser (1973)[13]pioneered both the HFP and MDB tasks. He recommends a flicker rate of 15- 20 Hz for the HFP task[14]. Macular pigment can be measured at that flicker rate using a blue background, because the participation of the s-cones and rods are excluded[15]. The MDB task avoids the exclusion of s-cones and rods due to flicker and is preferred by Kaiser (1971)[16]. Both methods were compared in this study. The HFP flicker rate was set to 8.3 Hz to conform to the CRT refresh rate and to maximize the opportunity to measure s-cone and rod input.

The Sony GDM-C520 CRT was scanned with an Ocean Optics USB2000 spectrophotometer and calibrated with a Minolta CS100A spot color meter. The spectral sensitivity of the receptors is plotted with the output of the phosphors in Figure 1. All four of the color standards had a

photopic Y of 18.9 cd/m². That was the maximum luminance available from the pure red phosphor, so the pure red stimuli were set to RGB= 255,0,0. The pure green stimuli were also set to 18.9 cd/m² (RGB= 0, 158, 0). The pure blue phosphor was only able to provide a maximum luminance of 6.8 cd/m², so it was necessary to add enough of the another phosphor to match the equiluminance of 18.9 cd/m²: RGB= 211,0,255 for the blue & red stimuli and RGB= 0,130,255 for the blue & green stimuli. All of the neutral stimuli were set to the chromaticity of Illuminant D (x= 0.313 and y= 0.328). There were 74 neutral (achromatic) stimuli chosen varying in luminance between photopic Y= 1.8 and 35.3 cd/m².

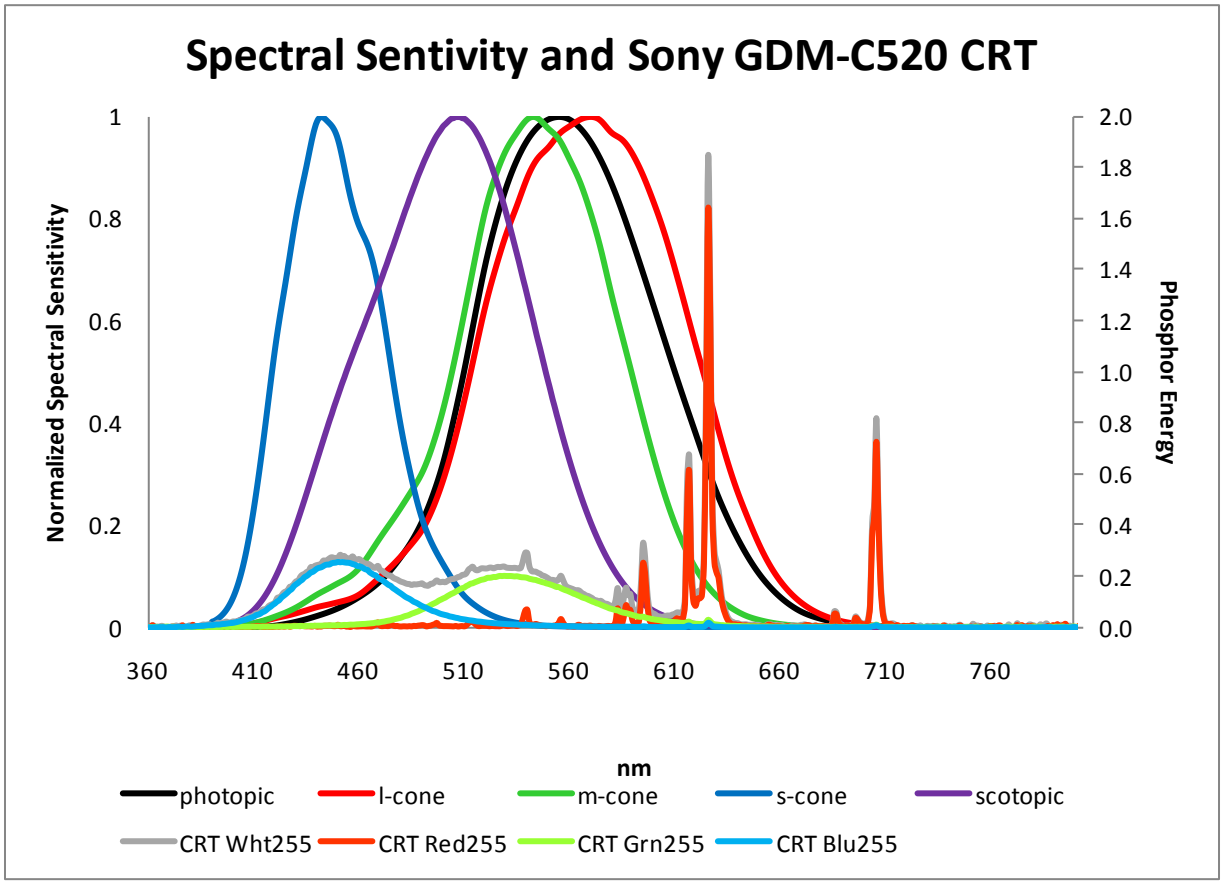

Figure 1 Spectral sensitivity of the receptors compared to the output of the phosphors

In order to avoid unintended chromatic shifts, neutral density gels sandwiched between acrylic panels were interposed between the CRT and the participant in order to reduce available luminance. The acrylic panels with no gel were used for the baseline condition and transmitted 97% of the display. Seven other panels were constructed in 0.6 OD steps (transmittance= 0.25000, 0.0625, 0.01563, 0.00391, 0.00098, 0.00024, and 0.00006). For the equiluminance chromatic stimuli, that produced a range between 18.3 and 0.001 cd/m^2. That effectively spanned the mesopic range (10 to 0.01 cd/m^2).

2.2.3 Procedure

Each session lasted less than two hours. After screening and instructions, the participant adapted for 15 minutes by playing a video game on a monochromatic monitor filtered to 35 cd/m² in a light proof lab. The gels were always run from highest transmittance to lowest transmittance in order to maintain adaptation. The experimenter used a night vision goggle (ATN NVG7) to control the experiment at the lower luminance levels. Within a gel, the HFP trials preceded the MDB trials. Within the HFP trials, the sizes were run from small to large. The order of the four color standards was counterbalanced across trials within each size of the HFP trials and within the MDB trials.

A VisualBasic interface provided a slider control of the neutral stimulus to the participant. For the specific color standard presented on a given trial, the participant chose which of the 74 neutral (achromatic) stimulus luminances minimized the flicker or border on the HFP and MDB task, respectively. In order to prevent set effects, the initial neutral stimulus was randomly varied between trials within the range of 11.22- 26.55 cd/m².

2.3 Results

Each individual's final neutral match setting was converted to its unfiltered photopic Y. The data were very noisy. As noted above, three participants were replaced. For each task, color standard, size, and luminance combination, individual data outside 5 standard errors of the mean (13.2%) were excluded from further analysis. Figures 2 and 3 show the mean neutral Y and standard error of the mean for each of the four color standards as a function of luminance for each color standard size combination in each task. All four of the color standards had a photopic Y of 18.9cd/m². Had vision remained photopic across the mesopic range, an ideal observer would have always set the neutral match to 18.9cd/m² (shown as the horizontal black line in the figures). The pattern of deviations from the line for the four color standards at a specific luminance can be used to estimate relative photoreceptor efficiency. Changes in those patterns with luminance reflect changes in photoreceptor efficiency across the mesopic range.

It should be recalled from Figure 1 that each of the 2-degree cone fundamentals of Stockman and Sharpe (2000)[17], the CIE 2-degree photopic luminosity curve (1924), and the CIE scotopic luminosity curve (1951) were normalized with a peak of 1.0. Each visual sensitivity was convolved with each of the phosphor scans to determine the normalized illuminance that each photoreceptor would capture. Those photoreceptor absorption figures were then used to compute the unfiltered weight of each photoreceptor for each of the four fixed color standards. Those same photoreceptor absorption figures were also used to compute the unfiltered weight of each photoreceptor for the mean neutral matching stimulus for each task, color standard, size, and luminance combination. All photoreceptor fundamentals are normalized with a peak of 1.0, but the weights were derived using photopic Y with a peak at 555 nm. The normalization process inflates the weight of both shorter and longer wavelengths and the photoreceptors selective for those wavelengths. Consequently the weights (especially for the rods and s-cone) can exceed the mean photopic Y (18.9).

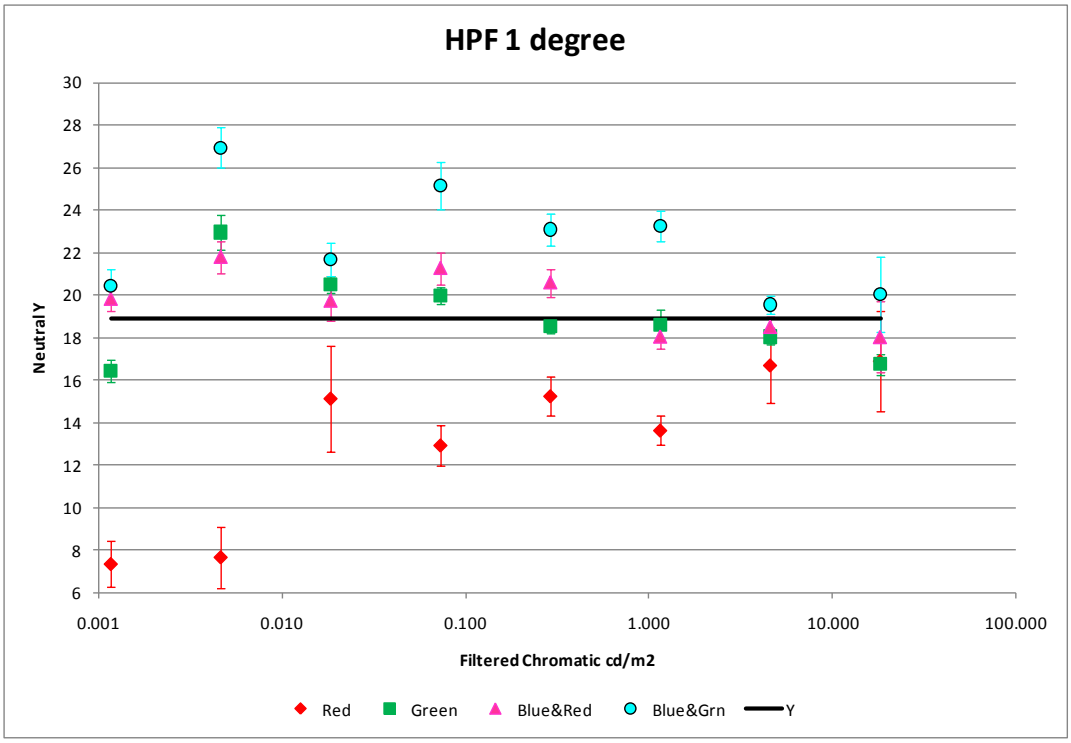

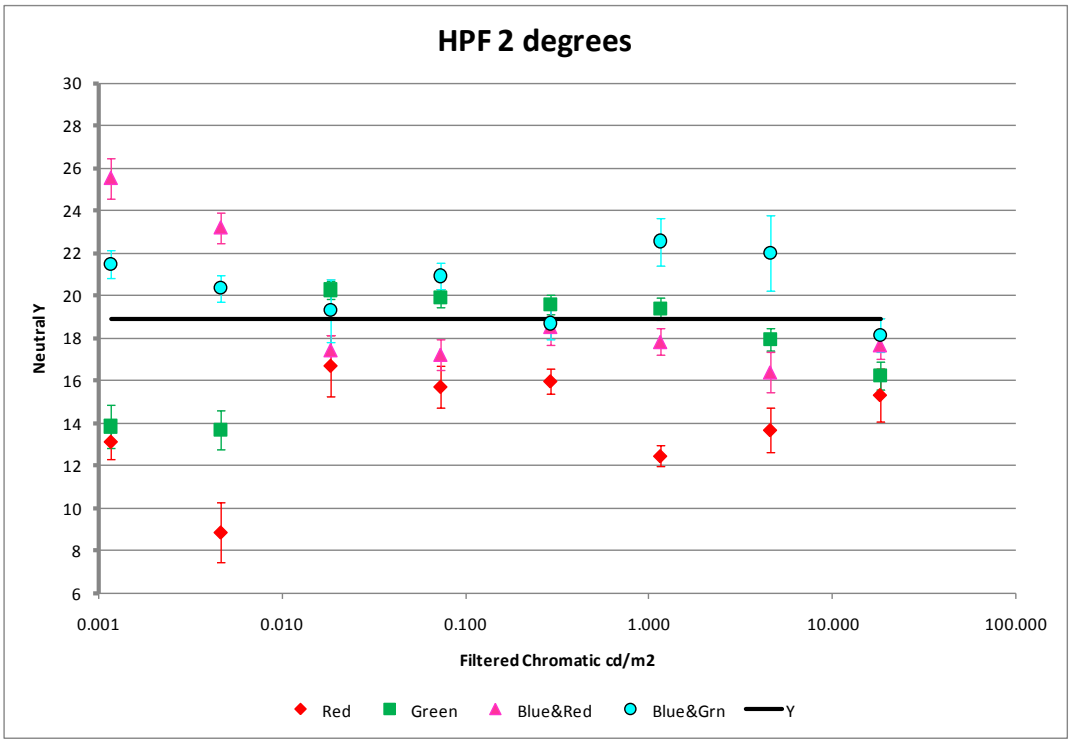

Figure 2 (a &b) Mean neutral Y for the 1 and 2 degree stimuli in the HPF task

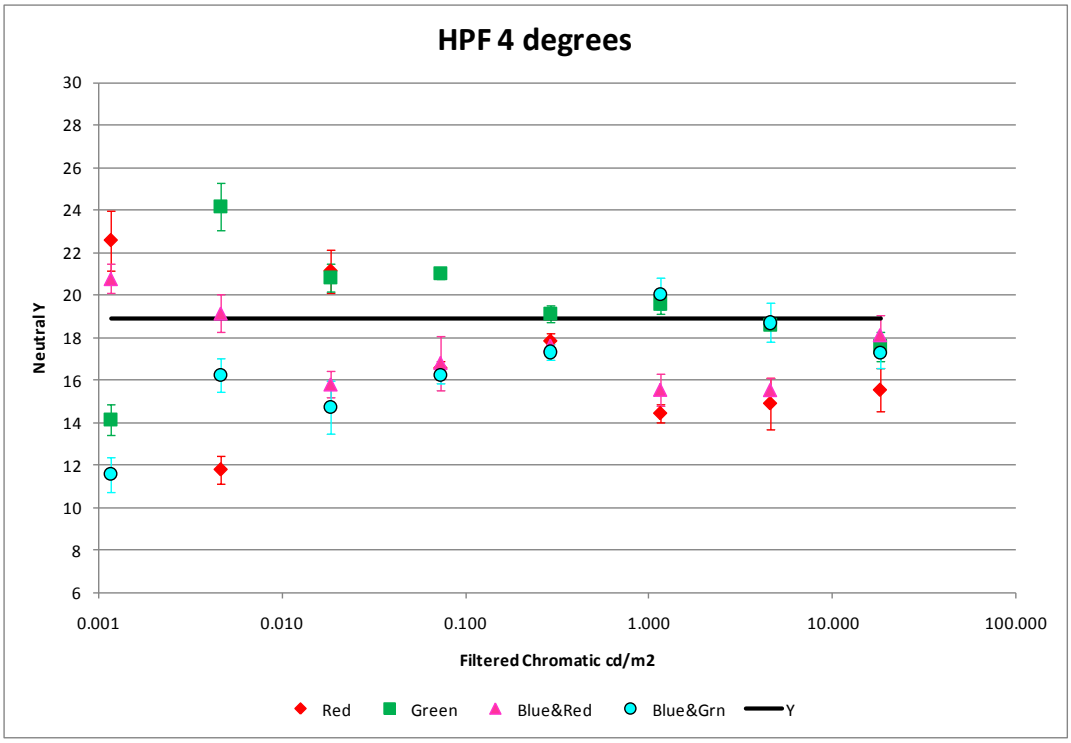

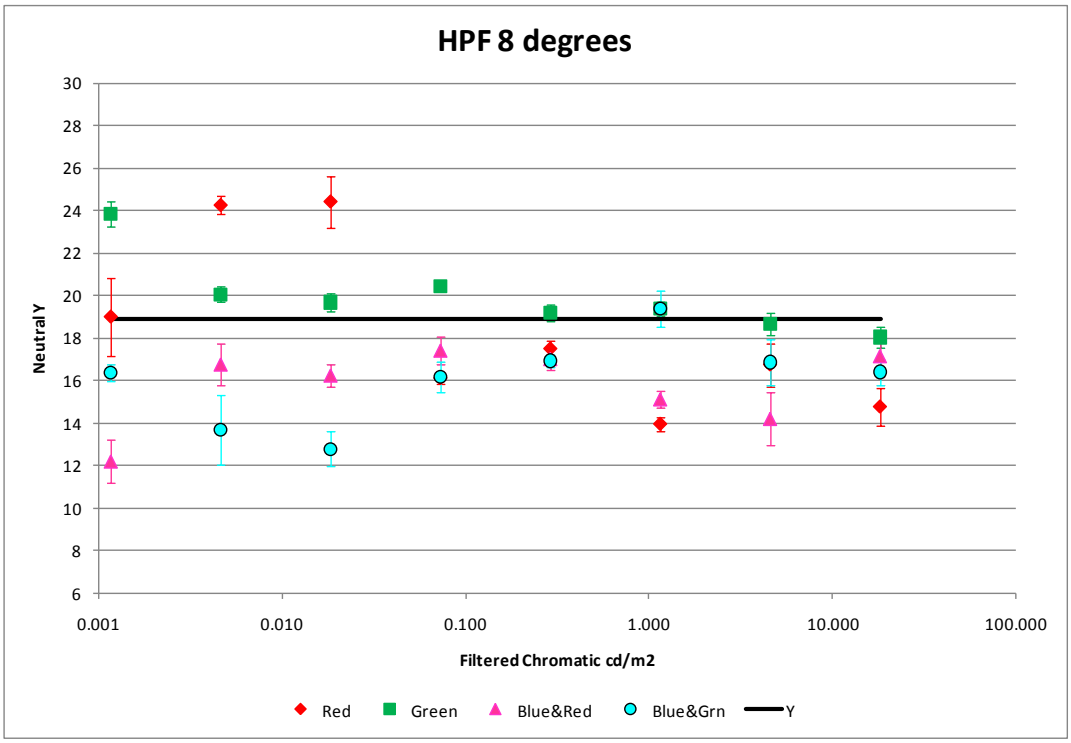

Figure 2 (c & d) Mean neutral Y for the 4 and 8 degree stimuli in the HPF task

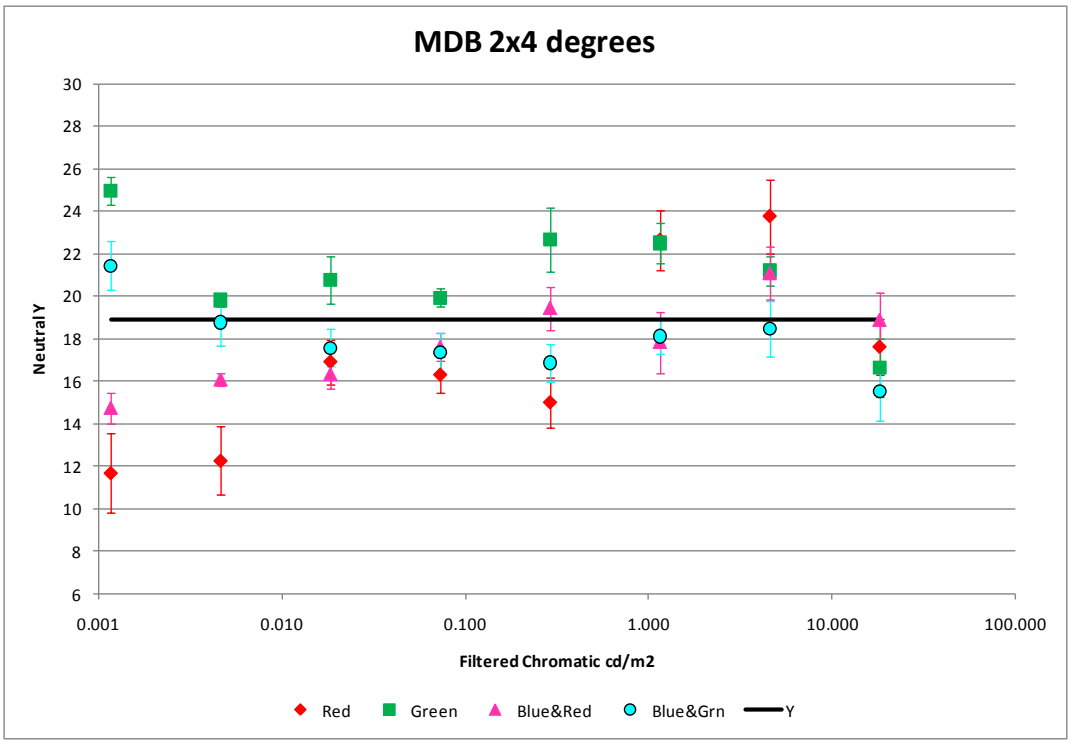

Figure 3 Mean neutral Y for the stimuli in the MDB task (the bipartite square was 4 X 4 degrees)

As a function of stimulus color, the l-cone weights and m-cone weights are almost perfectly negatively correlated (r= -0.909). Also, the s-cones and rods are almost perfectly positively correlated (r= 0.939). The s-cones are slightly negatively correlated with the l-cones and moderately positively correlated with the m-cones (r= 0.537). The correlations are stronger for the rods: r= -0.470 for the l-cones and 0.795 for the m-cones. The negative correlation between the l- and m-cones can be used to determine their relative contributions as a function of filtered stimulus luminance. Figure 4 shows the correlations of the l-cone and m-cone weights with matching neutral Y chosen across the four standard colors. The l-cone correlation always goes negative by 1.1 cd/m² in the HFP task ((it was negative at 4.5 cd/m² for the 2 degree stimuli) and was well below the m-cone correlation at 0.29 cd/m² in the MDB task.

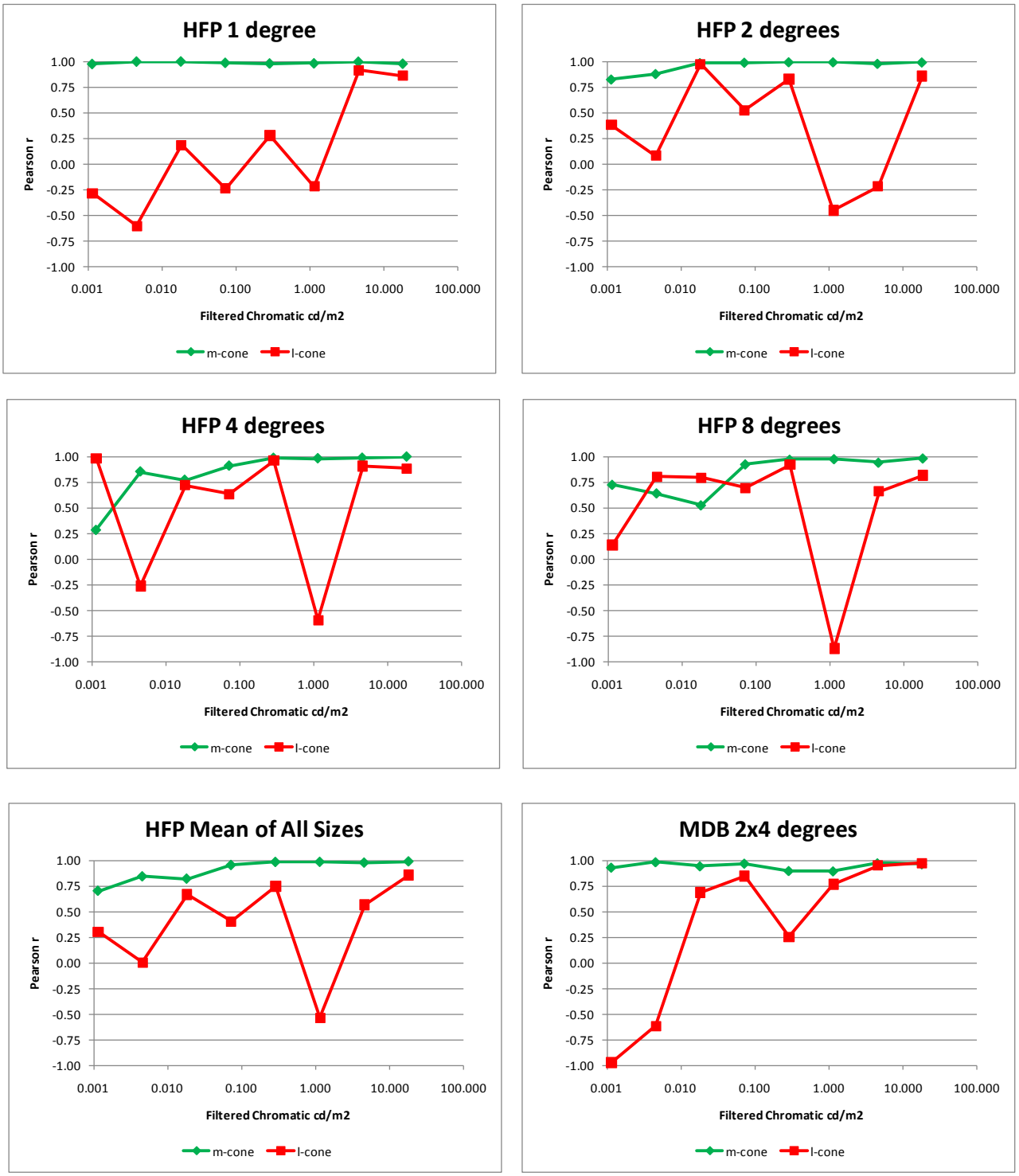

Figure 4 Correlations of the l-cone weights and the m-cone weights with matching neutral Y chosen across the four standard colors as a function of filtered luminance

These data indicate that the l-cone contribution is less important than the m-cone contributions below about 1 cd/m². It should be noted that the l-cone correlations tend to approach the m-cone correlations again in the luminance range between 0.29 and 0.018 cd/m² and then drop again at the lowest luminance levels.

Figure 5 again shows the m-cone correlations, but here they are compared to the s-cone and rod correlations. As can be seen, the s-cone and scotopic correlations are very high and very similar across the luminance range for both tasks and all sizes. The m-cone contribution remains high across the luminance range for the 1 degree targets in the HCP task. Relative to the s-cone and scotopic contributions, the m-cone contribution drops out at higher luminances as stimulus size increases in the HCP task: below 0.07 cd/m² for the 2 degree stimuli, below 0.29 cd/m² for the 4 degree stimuli, and below 1.14 cd/m² for the 8 degree stimuli. Averaging across the HFP sizes, the m-cone contribution is diminished below 0.07 cd/m². For the temporally constant 2 x 4 degree stimuli in the MDB task, the m-cone contribution is diminished below 4.53 cd/m². It then recovers before dropping again below 0.07 cd/m². It is difficult to distinguish between s-cone and scotopic contributions given the nearly perfect correlation between their weight and their uniformly high correlations with matching neutral Ys for the color standards across the filtered luminance range. Since the lowest filtered luminance levels were scotopic in this study, those contributions must be due to rods.

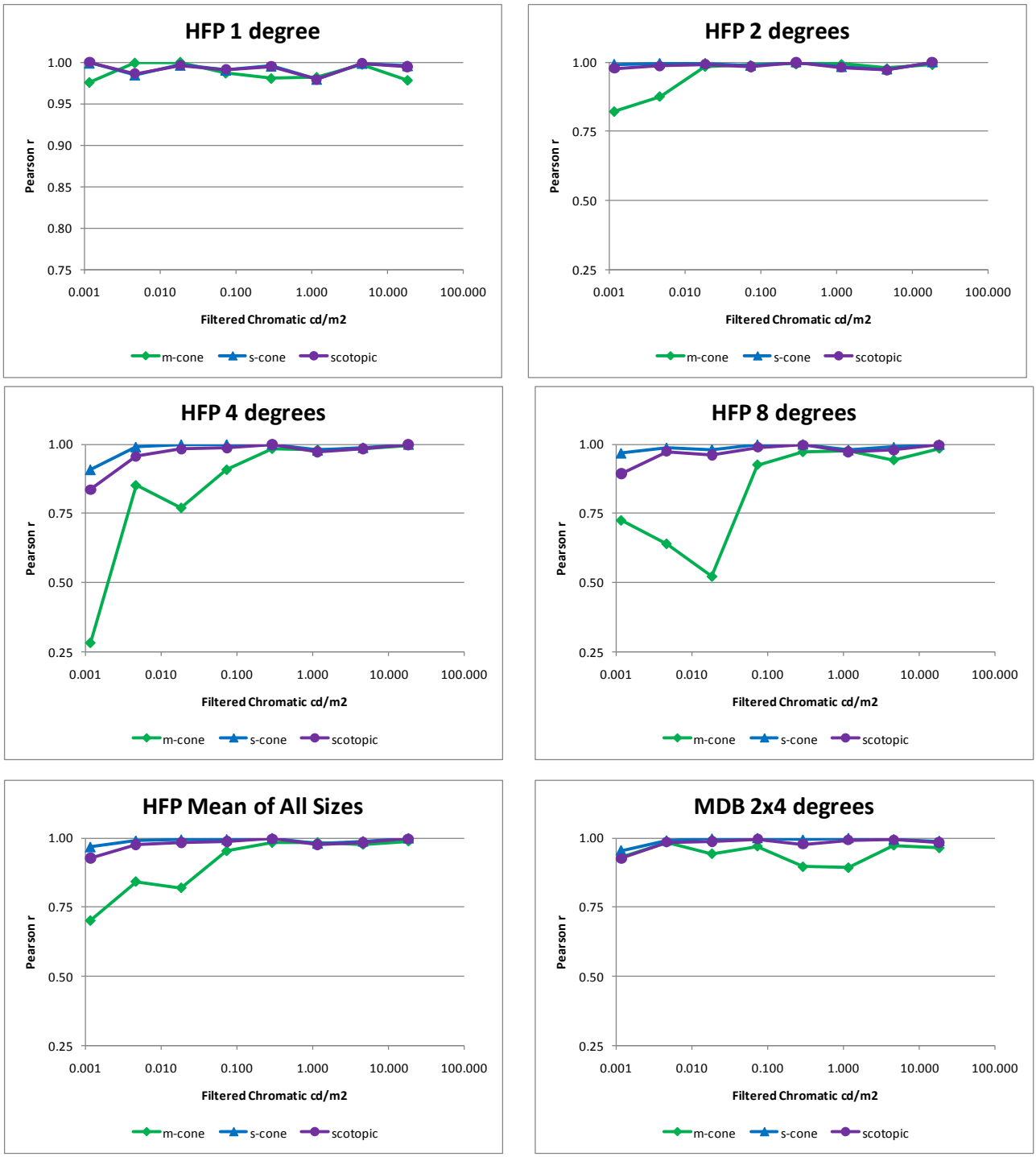

Figure 5 Correlations of the m-cone, s-cone, and rod weights with matching neutral Y chosen across the four standard colors as a function of filtered luminance

2.4 Conclusions

The l-cone contribution was considerably less than the m-cone contribution at 1.16 cd/m² for all sizes in the HFP task. There is a hint that the magnitude of the l-cone drop off at 1.16 cd/m² increases with stimulus size, but the data are far too noisy to draw a firm conclusion. In the MDB task, the drop off is less and does not occur until filtered luminance was reduced to 0.29 cd/m².

While the m-cone has a stronger contribution than the l-cone in the mesopic range, the m-cone contribution generally fell below the rod (and/or s-cone) contribution as luminance decreased. Consistent with the previous literature, s-cone and rod contributions were reduced for the temporally modulating HFP stimuli (even at 8.3 Hz) and for the smaller stimuli. Ignoring the size effect, the m-cone contribution fell below the rod (and/or s-cone) contribution below 0.07 cd/m² in the HFP. Being temporally constant, the moderately large stimuli (each bipartite field subtended 2x4 degrees of visual angle) in the MDB task should provide a benefit for the s-cones relative to the m-cones. The first drop off of the m-cones by 1.15 cd/m² is consistent with that Interpretation.

In a recent study, Raphael & MacLeod (2008)[18] compared cone and rod contributions in a MDB task. They reported a transition from cones to rods at 0.05 cd/m². In this MDB task, the m-cone contribution approached the rod (and/or s-cone) contribution at 0.07 cd/m² and then dropped again. It was earlier noted that the l-cone and m-cone correlations converged in the luminance range between 0.29 and 0.018 cd/m² before subsequently diverging. These data support the conclusions of Raphael & MacLeod.

3. EXP2 & 4: CONTRAST SENSITIVITY AND CONTRAST ACUITY FOR REGAN LETTERS

3.1 Rationale

While Experiment 1 investigated changes in relative photoreceptor sensitivities across the mesopic range, Experiments 2 and 4 investigated changes in the relative importance of the photoreceptors for contrast acuity and contrast sensitivity across the mesopic range. The photopic luminosity function predicts contrast acuity and sensitivity within the photopic range. This reflects the higher spatial sensitivity of the luminance channel compared to the color-opponent channels[19]. Based on the rods, the scotopic luminosity function similarly predicts contrast acuity and contrast sensitivity within the scotopic range. As demonstrated in Experiment 1, relative photoreceptor sensitivities change across the mesopic range. Will those changes also be reflected in contrast sensitivity and acuity? Will adaptation to an achromatic display (Experiment 2) produce a different set of results than adaptation to a green display simulating a night vision goggle (Experiment 4)?

3.2 Method

3.2.1 Participants

Twelve participants were recruited for each of Experiments 2 and 4. All passed the screening and were included for data analysis. In Experiment 2, there were eight male and four female participants with a mean age of 21.3 years (18- 28). In Experiment 4, there were eight male and four female participants with a mean age of 21.0 years (18- 29).

3.2.2 Design and Stimuli

As in Experiment 1, all 24 participants first adapted for 15 minutes by playing a video game on a monochromatic monitor filtered to 35 cd/m² in the light proof lab. For the 12 participants in Experiment 2, the monochromatic display was filtered by a neutral density filter. A green filter simulating a night vision goggle display was used to filter the monochromatic display for the 12 participants in Experiment 4. Other than the adaptation filter manipulated between the group of participants in Experiments 2 and 4, the two experiments had exactly the same design and will be discussed together.

Each experiment was a within-subject design. The two tasks were Regan letter contrast acuity and Regan letter contrast sensitivity. Pilot testing was used to subsample relevant stimuli within the 256 possible combinations of 8 filtered luminances X 4 photoreceptor colors X 4 contrasts (for contrast acuity) & 4 sizes (for contrast sensitivity) for each of the two tasks. Across the two tasks, only 96 combinations could be tested within the 2-hour session. Based on the pilot test, 54 combinations were chosen for the contrast acuity task and 42 combinations were chosen for the contrast sensitivity task.

All stimuli were presented on the same Sony GDM-C520 CRT described in Experiment 1. The same 8 acrylic gel sandwiches used in Experiment 1 were used in this experiment, but all unfiltered stimulus displays were set to photopic Y= 35 cd/m². Consequently, the 8 luminances viewed by the participants were: 33.95, 8.53, 2.14, 0.54, 0.135, 0.034, 0.009, and 0.002 cd/m². The stimuli were letters based on prototypes generated by Bill Brockmeier (AFRL/RHDO) from the font Regan used in his contrast acuity charts. Each letter was chromatic on a neutral, achromatic background of the same luminance. The background was equivalent to an illuminant D (x, y= 0.313, 0.328) at Y= 35 cd/m². The letters were also Y= 35 cd/m², but their chromaticities were chosen using the approach of Rabin (1996)[20]. He generated three cone – specific contrast sensitivity charts (l-cone, m-cone, and s-cone). Within each chart, the contrast between the chromatic letters and the back ground was systematically reduced across rows while holding luminance contrast and contrast for the other two cone as low as possible. Following his procedure, eight specific contrasts were generated for the three cones and for rods using equation 13 from Cole & Hine (1992)[21], the calibrations from the Sony GDM-C520 CRT, the 2-degree cone fundamentals of Stockman and Sharpe (2000) , and the CIE scotopic luminosity curve (1951). Consistent with Rabin, the –cone and m-cone contrasts were closely matched and the selected s-cone contrasts were higher due to their lower density in the retinal mosaic. For this study, the rod contrasts selected closely matched the s-cones. This will allow direct comparisons between the l- and m-cone importance and the between the s-cone and rod importance. Figure 6 shows the photoreceptor-specific contrasts (log(Percent)) for the eight rows in the contrast

sensitivity charts. The contrast for the other photoreceptors is also included to show that the specific photoreceptor contrast is higher than for the other photoreceptor contrasts for each chart.

For the contrast acuity task, 16 "charts" were created to present on the CRT. All of the letters on a chart were one of the four photoreceptor-specific colors. All of the letters on a chart were one of four possible contrasts for that color. For the l- and m-cone charts, the contrasts were 5.3%, 7.6%, 11.5%, & 20.7% and 5.2%, 7.6%, 11.4%, & 20.7%, respectively. For the s-cone and rod charts, the contrasts were 15%, 22%, 33%, and 60%. As with Regan's charts, there were 11 lines on each chart with the largest letters on the top row. Progressively lower rows contained letters with progressively smaller stroke widths. Viewed from 86.7 cm, the stroke widths were 20.1, 16.1, 12.1, 10.1, 9.0, 8.0, 6.0, 5.0, 4.0, 3.0, and 2.0 minutes of arc (Snellen equivalents= 402, 322, 241, 201, 181, 161, 121, 101, 80, 60, and 40). To control letter confusability, each row included the letters R, K, N, and H (confusable); either C & O or D & O (also confusable); and two of V, Z, and S (distinctive). The order of letters in a row was counterbalanced across rows and charts.

For the contrast sensitivity task, another 16 "charts" were created. Each was a single photoreceptor-specific color. Figure 6 shows the contrast of the letters in each of the eight rows. All of the letters in a chart were the same size: either stroke width of 3, 5, 10, or 20 minutes of arc (Snellen equivalents of 60, 101, 201, or 402). The composition and order of the eight letters in each row conformed to the same rules described above.

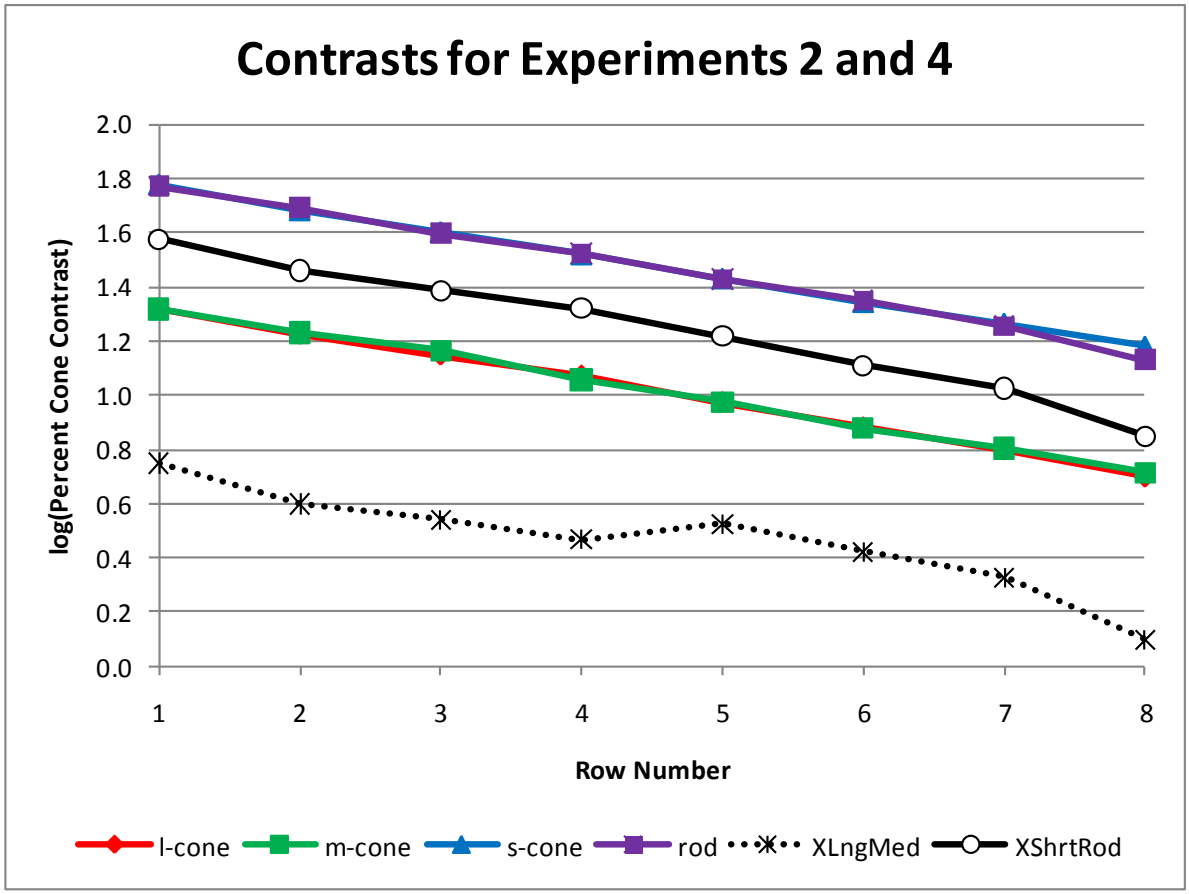

Figure 6 Photoreceptor contrast (log(Percent)) as a function of each row in each contrast sensitivity chart in Experiments 2 and 4. Contrast for the other photoreceptors is also shown for comparison

3.2.3 Procedure

As noted above, only 96 charts of the possible 256 combinations of 16 charts and eight luminance levels could be presented to the participant in the two-hour session. The principle investigator and two research assistants tested each other in a pilot test. The pilot test identified the charts most likely to include a threshold at each luminance level. Those 96 combinations consisted of 54 contrast acuity chart/luminance combinations (see Table 1) and 42 contrast sensitivity chart/luminance combinations (see Table 2).

Table 1 Contrast Acuity charts presented at each unfiltered luminance in Experiments 2 and 4.

Luminance	33.950	8.528	2.142	0.538	0.135	0.034	0.009	0.002
l-c 5.3%	l-c 5.3%	l-c 5.3%	l-c 5.3%					
l-c 7.6%	l-c 7.6%	l-c 7.6%	l-c 7.6%	l-c 7.6%				
l-c 11.5%		l-c 11.5%	l-c 11.5%	l-c 11.5%	l-c 11.5%			
l-c 20.7%			l-c 20.7%	l-c 20.7%	l-c 20.7%			
m-c 5.2%	m-c 5.2%	m-c 5.2%						
m-c 7.6%	m-c 7.6%	m-c 7.6%						
m-c 11.4%	m-c 11.4%	m-c 11.4%	m-c 11.4%					
m-c 20.7%		m-c 20.7%	m-c 20.7%	m-c 20.7%				
s-c 15%		s-c 15%	s-c 15%	s-c 15%				
s-c 22%			s-c 22%	s-c 22%	s-c 22%			
s-c 33%			s-c 33%	s-c 33%	s-c 33%	s-c 33%		
s-c 60%				s-c 60%	s-c 60%	s-c 60%	s-c 60%	
rod 15%		rod 15%	rod 15%	rod 15%	rod 15%			
rod 22%			rod 22%	rod 22%	rod 22%	rod 22%		
rod 33%				rod 33%	rod 33%	rod 33%	rod 33%	
rod 60%					rod 60%	rod 60%	rod 60%	rod 60%

Table 2 Contrast Sensitivity charts presented at each unfiltered luminance in Experiments 2 and 4.

Luminance	33.950	8.528	2.142	0.538	0.135	0.034	0.009	0.002
l-c 3	l-c 3							
l-c 5	l-c 5	l-c 5						
l-c 10		l-c 10	l-c 10	l-c 10	l-c 10			
l-c 20				l-c 20	l-c 20	l-c 20		
m-c 3	m-c 3							
m-c 5	m-c 5							
m-c 10	m-c 10	m-c 10	m-c 10					
m-c 20		m-c 20	m-c 20	m-c 20	m-c 20			
s-c 3	s-c 3	s-c 3						
s-c 5	s-c 5	s-c 5	s-c 5					
s-c 10			s-c 10	s-c 10	s-c 10	s-c 10		
s-c 20					s-c 20	s-c 20	s-c 20	
rod 30	rod 3	rod 3						
rod 5		rod 5	rod 5					
rod 10				rod 10	rod 10	rod 10		
rod 20					rod 20	rod 20	rod 20	rod 20

The general procedures were similar to Experiment 1. Each session lasted less than two hours. The participant adapted for 15 minutes by playing the video game and then the gels were run

from highest transmittance to lowest transmittance in order to maintain adaptation. Within a gel, the contrast acuity trials preceded the contrast sensitivity trials. Within each task, the photopic-specific color order was counter-balanced between gels. Within a color, the contrast acuity trials were run from highest contrast to lowest and the contrast sensitivity trials were run from largest stroke width to smallest. The goal was to help these novice observer's learn the task. Within a chart, the observer started with the hardest row that could be accurately identified. Then the observer progressed through more and more difficult rows until no letter could be identified. Partial rows were combined to compute a single acuity or contrast score for each chart. Again the experimenter used a night vision goggle to control the experiment and record the data at the lower luminance levels.

3.3 Results

3.3.1 Contrast acuity.

logMAR was computed for each chart at each filtered luminance for each participant. Then the mean logMAR across participants was computed for each chart at each filtered luminance. As previously noted, the contrasts were matched for the l- and m-cones and the contrasts were matched for the s-cones and rods. Photoreceptor sensitivity (1/contrast) was computed for the logMAR stimuli. A multiple regression in SPSS was performed for the logMARs for all charts within each luminance level using l-cone contrast and m-cone contrast. A similar multiple regression was run for s-cone contrast and rod contrast. Irrespective of adaptation color, l-cone contrast was more important than m-cone contrast at 33.96 cd/m². M-cone contrast was more important than l-cone contrast at all lower filtered luminances (starting at 8.52 cd/m²). S-cone contrast was more important than rod contrast at 33.95 and 8.83 cd/m². Rod contrast was more important than s-cone contrast at lower filtered luminances (starting at 2.14 cd/m²). Based on these results, m-cone and rod sensitivities are the better predictors of logMAR at 2.14 cd/m² and below. A multiple regression was run for m-cone and rod sensitivities for that range. Given the greater range of rod contrasts in the design, it is hardly surprising that rod sensitivity was the better of the two predictors. What is important is that m-cone sensitivity remained an important and independent predictor of logMAR after partialing out rod sensitivity down to 0.135 cd/m². For 0.034 and lower filtered luminances, only rod sensitivity was relevant. In short, the two best predictors at 33.95 cd/m² were l-cone and s-cone sensitivities. At 8.53 cd/m², the two best predictors were m-cone and s-cone sensitivity. From 2.14 cd/m² through 0.135 cd/m², m-cone and rod sensitivities were the best predictor. From 0.034 through 0.002 cd/m², only rod sensitivity was relevant. The intercept and betas for the best two predictors (above 0.034 cd/m²) were tested for fit. Figure 7 shows the multiple regression intercepts plotted against the filtered log luminance. The fits are generally very good, but the intercepts for 33.95 cd/m² are too high (estimated sensitivity is too low). Some of the observers were able to read all of the letters on some charts at 33.95 cd/m², so contrast acuity is underestimated. While the best-fit slopes are virtually identical for the white adaptation (Experiment 2 and green adaptation (Experiment 4) participants, the best-fit intercept is slightly higher with green adaptation than with white adaptation. Ignoring the 33.95 cd/m² point, the difference only approaches statistical significance; $t(6)= 2.32$; $p= .060$). The slight advantage in sensitivity with white adaptation is marginal at best. Figure 8 compares the predicted logMAR values to the observed logMAR

values after setting the fit intercept to 0. Both fits are good with slopes very close to unity. There is no difference between white and green adaptation.

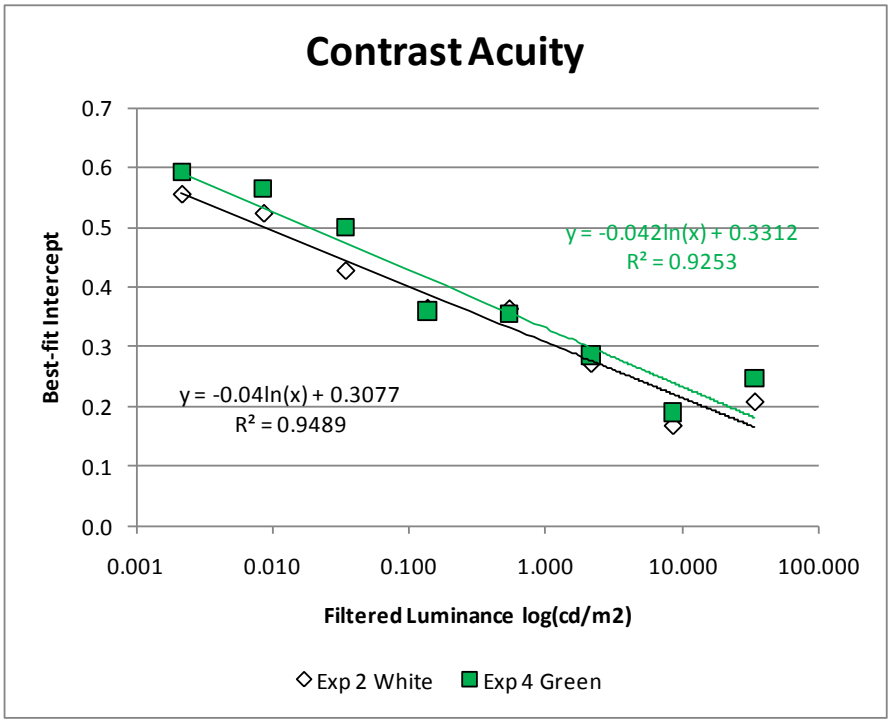

Figure 7 The best-fit intercepts for contrast acuity in Experiments 2 and 4

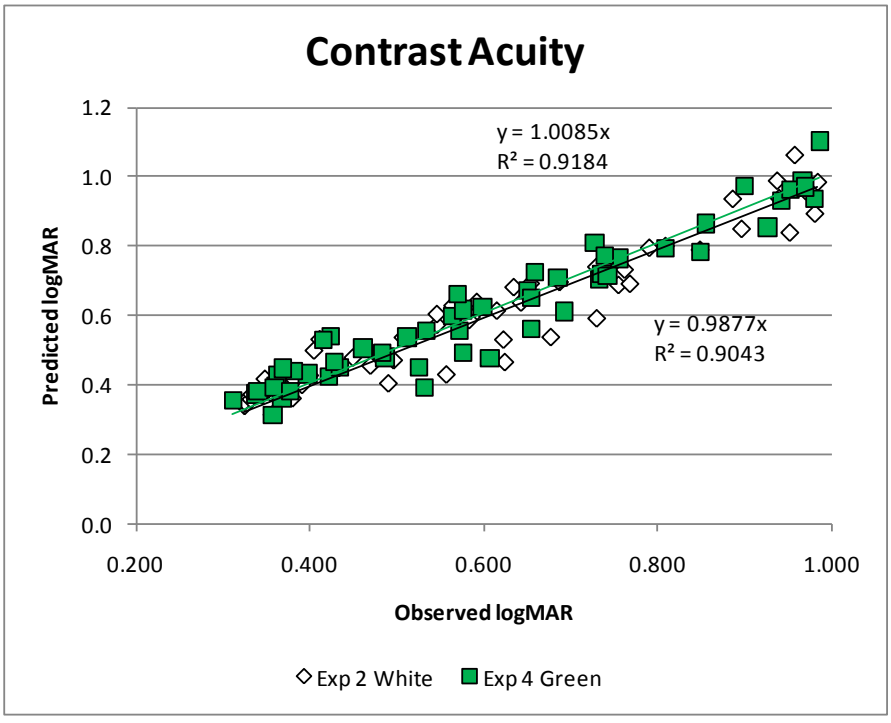

Figure 8 The best-fit model using two best predictors and intercept set to 0 for Experiments 2 and 4

3.3.2 Contrast sensitivity

While contrast acuity measures the smallest letters that can be recognized at a particular contrast, contrast sensitivity measures the letters of a particular size that can be recognized at the lowest contrast. Partially correct lines were combined to compute minimum contrast (most sensitive) for each participant for each chart viewed at each filtered luminance. Means were computed across the 12 participants in each experiment. As shown in Table 2, not all sizes were tested at all filtered luminance levels (e.g.; the largest stimuli were not tested at the highest luminance). For those size and luminance combinations that had been tested, TableCurve3D was used to fit minimum contrast with l-cone and m-cone contrasts. In four combinations, both l-cone and m-cone contrasts were important and the l-cone contrast was the better predictor. For the other 14 combinations, only the m-cone contrast was relevant. Since there was no evidence of adaptation filter; the mean contrast across all 24 participants of Experiments 2 and 4 was computed. Mean contrast was converted to contrast sensitivity (1/contrast). The results for the l-cone and m-cone contrast sensitivities are shown in Figure 9. L-cone contrast sensitivity was only superior to m-cone contrast sensitivity for large targets at high luminance levels: the 20s minute of arc letters at and above 0.54 cd/m² and the 10 minutes of arc letters at 8.53 cd/m² (hidden under the 20 minutes letter data point in the graph). In the photopic range, the data suggest that m-cone contrast sensitivity is a band-pass function of size (consistent with the standard contrast sensitivity function). Below 0.54 cd/m², m-cone contrast sensitivity is higher for larger stimuli. The m-cone contrast sensitivity remains robust for the larger (10 and 20 minutes of arc) letters even at low filtered luminance levels. A similar analysis was performed for the s-cone and rod data. Those contrast sensitivities are shown in Figure 10. Compared to the s-cones, rods have superior contrast sensitivity at the lowest filtered luminance levels (below 0.034 cd/m²). At and above 2.14 cd/m², the s-cones have much higher contrast sensitivity for the large stimuli (20 minutes of arc stroke width). Surprisingly, there was evidence of rod contrast sensitivity in the photopic range for smaller stimuli.

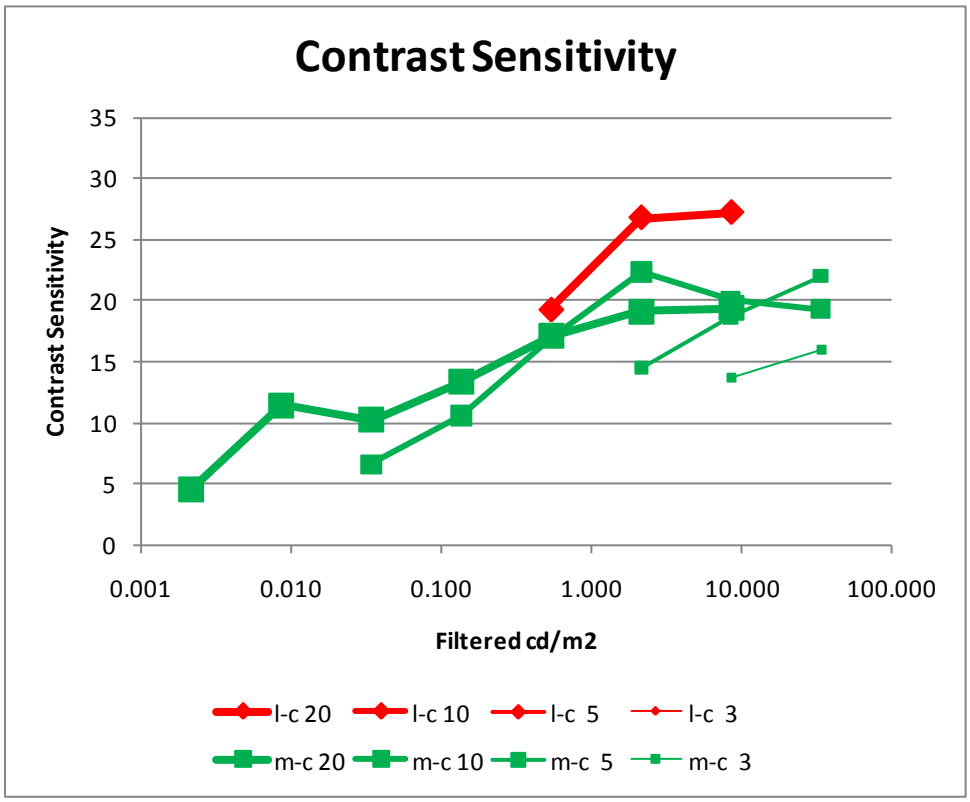

Figure 9 L-cone and m-cone contrast sensitivities in Experiments 2 and 4

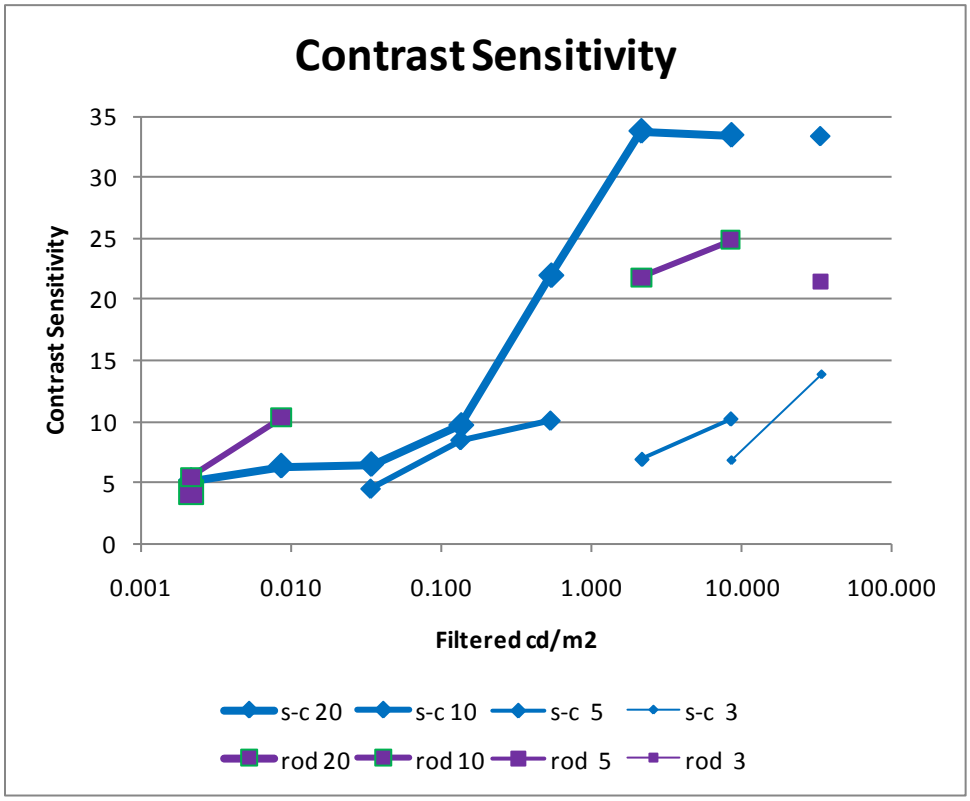

Figure 10 S-cone and rod contrast sensitivities in Experiments 2 and 4

3.4 Conclusions

Consistent with Experiment 1 and with the results of Raphael & MacLeod (2008), only rod input was relevant for contrast acuity at and below 0.034 cd/m². Only rod input was relevant for contrast sensitivity below 0.034 cd/m². While l-cone contrast was more important than m-cone contrast for acuity at 33.96 cd/m², m-cone contrast was more important for the rest of photopic and mesopic range. In terms of contrast sensitivity, l-cone input was more important than m-cone input only for large letters. It will be recalled from Experiment 1 that m-cones dominated l-cones in the HFP task except at the highest filtered luminance levels and for the smallest size (1 degree). For Experiments 2 and 4, the "large" stimuli had a stroke width of 20 minutes of arc. Taken together, these data suggest a band-pass function of size (as was evident in the m-cone contrast sensitivity data). Consistent with Experiment 1, s-cone contrast sensitivity was low for the small stimuli. On the other hand, the importance of s-cone input for contrast sensitivity for large letters down to 0.038 cd/m² was very surprising.

The goal of manipulating adaptation color between Experiments 2 and 4 was to investigate concerns expressed by some aircrew after wearing NVGs for long periods of time. The green filter used in adaptation in Experiment 4 was chosen to simulate an NVG. There was no difference in the pattern of results due to adaptation filter and the slight fitted intercept advantage for achromatic adaptation only approached statistical significance. Adaptation was for 15 minutes in this study, so future research into this issue should use a much longer adaptation period.

4. EXP3: CONTRAST SENSITIVITY FOR GABORS

4.1 Rationale

Acuity is typically measured with letters or sinusoidal gratings. Both types of stimuli have hard edges (even at low contrast). Gabors are sinusoidal gratings convolved with a gaussian. Obviously their spatial frequencies can be directly mapped onto the spatial frequency of sinusoidal gratings and they can be directly related to the stroke width of letters. On the other hand, their convolution with a gaussian eliminates the hard edges in the other stimuli. That eliminates the confounding with odd higher spatial frequency harmonics and spatial frequencies normal to the grating. Therefore, gabors were used as the stimuli for this experiment.

4.2 Method

4.2.1 Participants

All 12 participants for Experiment 3 passed the screening and were included for data analysis. There were four male and eight female participants with a mean age of 19.5 years (18- 29).

4.2.2 Design and Stimuli

Experiment 3 was a 4 spatial frequencies (0.75, 1.5, 3, and 6 cpd) X 4 colors (red, green, blue & red, and blue & green) X 4 contrasts (80%, 40%, 20%, and 10% for the red and green gabors; 90%, 60%, 30%, and 15% for the blue & red and blue & green gabor's) X 8 filtered luminance levels (18.04, 4.53, 1.14, 0.286, 0.072, 0.018, 0.005, and 0.001 cd/m^2) repeated measures design.

The stimuli were gabors presented by a Cambridge Research System ViSaGe on the same calibrated Sony GDM-C520 CRT described above. Viewed from a distance of 1 meter, each gabor was generated in a square window that subtended 7.27 degrees of visual angle on a side (1/3 of screen width) and had a standard deviation of 1.17 degrees of visual angle (1/14 of screen height). As noted above, spatial frequency was varied between 0.75 and 6 cpd. All stimuli were equiluminant (Y= 18.6 cd/m^2), but varied in chromaticity. The red stimuli were the pure red phosphor at almost maximum power and the green stimuli were the pure green phosphor matched by the CRS ViSaGe to that same luminance. As in Experiment 1, the blue & red stimuli and the blue & green stimuli were created by adding enough of the red and green phosphors to the maximum blue phosphor to match the same luminance. Also, the neutral stimulus was again Illuminant D. The stimulus colors and the neutral point are shown as circles relative to the gamut in Figure 11. The photoreceptor chromaticities (based on Stockman & Sharpe (2000) and CIE (1951) scotopic luminosity function) are shown as circles in the figure. It should be noted that the monitor's green phosphor is matched to the m-cone. The l-cone is shifted less than 0.1 u' to the right of the green phosphor. The s-cone and rod chromaticities fall outside the monitor's gamut. The CRS ViSaGe used the neutral point coordinates, the color stimulus coordinates, and the contrast value to generate the gabor. The gabor varied that contrast percent around the midpoint between the neutral point and the color point. Stated differently, one gabor extreme was half the contrast percent of the distance toward the neutral point and the other gabor extreme was half the contrast percent of the distance toward the color point. While the same four

contrasts were used across pairs of colors, the variation in u'v' space differed. For instance, 80% contrast for a red gabor defined a longer vector than 80% contrast for a green gabor. As will be discussed below, the projection of those stimulus color vectors onto the photoreceptor vectors also differed. The same eight gels were used in this experiment to manipulate filtered luminance.

4.2.3 Procedure

Each session lasted about 90 minutes. The participant adapted for 15 minutes by playing the video game and then the gels were run from highest transmittance to lowest transmittance in order to maintain adaptation. Within a gel, the order of the colors was counterbalanced. Within a color, the gabor spatial frequencies were run from low (0.75 cpd) to high (6 cpd). Within each spatial frequency, the gabor contrasts were run from high (either 89% or 90%) to low (either 10% or 15%).

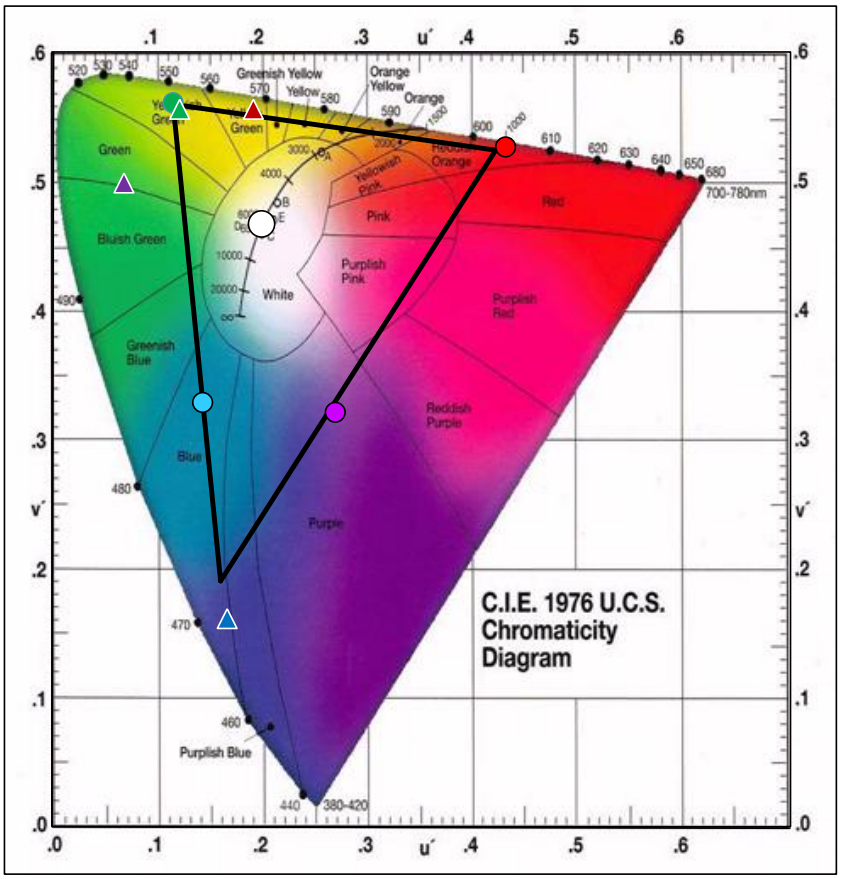

Figure 11 The neutral point and four colors (circles) used in Experiment 3. The photoreceptors (triangles) are also shown

On a given trial, three gabors of the same color, spatial frequency, and contrast were displayed laterally. They differed only in orientation. One was vertical, one was tilted 45° clockwise, and one was tilted 45° counterclockwise. If visible, the participant reported the orientations of the three gabors from left to right. Consequently, one could be guessed correctly by chance and three correct was perfect.

4.3 Results

The mean number correct of responses across the 12 participants was computed for each filtered luminance, gabor color, gabor spatial frequency, and gabor contrast. For each gabor color and spatial frequency, the threshold contrast was computed using the following algorithm. If accuracy was perfect across all participants and all contrasts, then threshold contrast was estimated as 1/12 (based on 12 participants) of the distance between 0 the minimum contrast tested. If accuracy was zero across all participants and all contrasts, then threshold contrast was estimated as 1/12 of the distance between 1and the maximum contrast tested. Threshold contrast was set to any contrast that produced accuracy exactly in between chance (1 correct) and perfect (3 correct). The remaining thresholds were interpolated between the nearest contrast above and below the midpoint between chance and perfect. Those threshold contrasts were then converted to threshold distances in u'v' space as was shown in Figure 11. Those threshold distances are shown in Figure 12. The u'v' distance between the neutral point and each 100% color point is also shown ("Max").

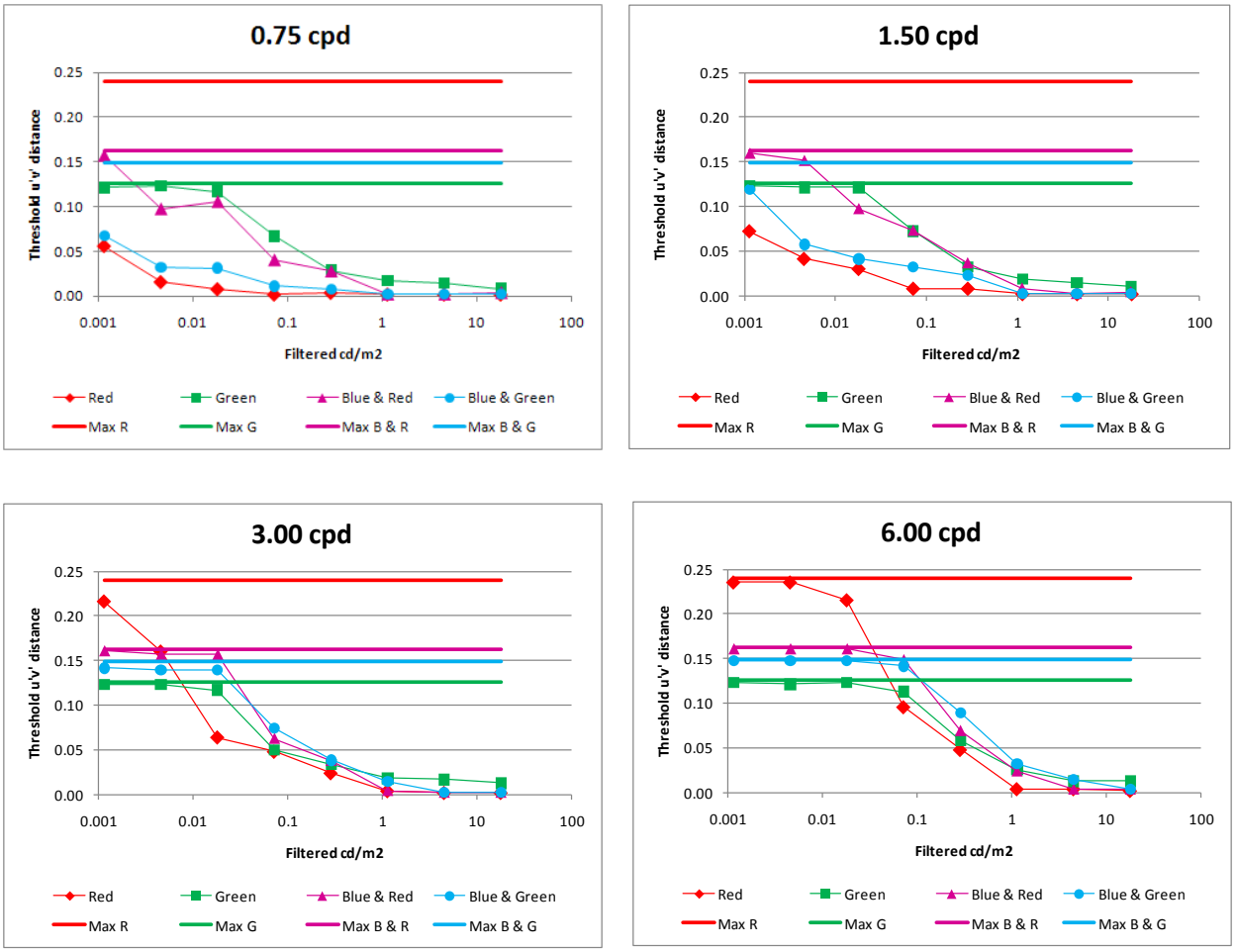

Figure 12 Threshold u'v' distances for the Experiment 3 gabors

The maximum possible shift in u'v' space for each color was then projected onto the vector between the neutral point and each of the photoreceptor coordinates shown in Figure 11. For each spatial frequency within each filtered luminance level, each photoreceptor projection for the fours colors was correlated with the threshold u'v' distance for the four colors. A photoreceptor's sensitivity should be evidenced by a negative correlation (smaller threshold u'v' distance relative to the largest photoreceptor projections). Those correlations (Pearson Product-Moment Coefficient) are shown in Figure 13.

For the 0.75 cpd gabors, threshold u'v' distances remained below ceiling for filtered luminances at and above 0.07 cd/m² (Figure 12). In that range, both l-cone and m-cone correlations were zero or positive (Figure 13). For the same range, s-cone correlations were negative at 1.14 cd/m² and above, while rod correlations were negative at and below 0.29 cd/m². For the 0.75 cpd gabors, the importance of s-cone input switched to rod input as filtered luminance was reduced from 1.14 cd/m² to 0.29 cd/m². For the 1.5 cpd gabors, threshold u'v' distances again remained below ceiling at and above 0.07 cd/m² (Figure 12) and the same pattern of correlations was found

in Figure 13: a) l-cone and m-cone correlations were zero or above and b) the switch from s-cones to rods occurred between 1.14 cd/m² and 0.29 cd/m². For the 3 cpd gabors, threshold u'v' distances again remained below ceiling at and above 0.07 cd/m² (Figure 12), but a different pattern of correlations was found in Figure 13. The m-cone correlations were negative at1.14 cd/m² and below. In addition, the switch from s-cones to rods now occurred at a higher filtered luminance (between 4.53 and 1.14 cd/m²) for these higher spatial frequency gabors. For the highest spatial frequency gabors (6 cpd), threshold u'v' distances only remained below ceiling for filtered luminances at and above 0.29 cd/m² (Figure 12). In that range, the m-cone correlations (Figure 13) were negative at and below 4.53 cd/m². The switch from s-cones to rods occurred at an even higher filtered luminance (between 18.04 and 4.53 cd/m²).

4.4 Conclusions

Even for the lowest spatial frequency gabors (0.75 cpd), threshold limits were encountered below 0.07 cd/m². That is close to the rod / cone breaks found in the MDB task of Experiment 1 (0.07 cd/m²) and in Experiments 2 & 4 (0.034 cd/m²). Consistent with the previous results, s-cone sensitivity dropped dramatically for the higher spatial frequency stimuli, but the s-cone to rod switch occurred at higher luminances in this experiment. The importance of m-cone input for higher spatial frequency targets is also consistent with the previous results.

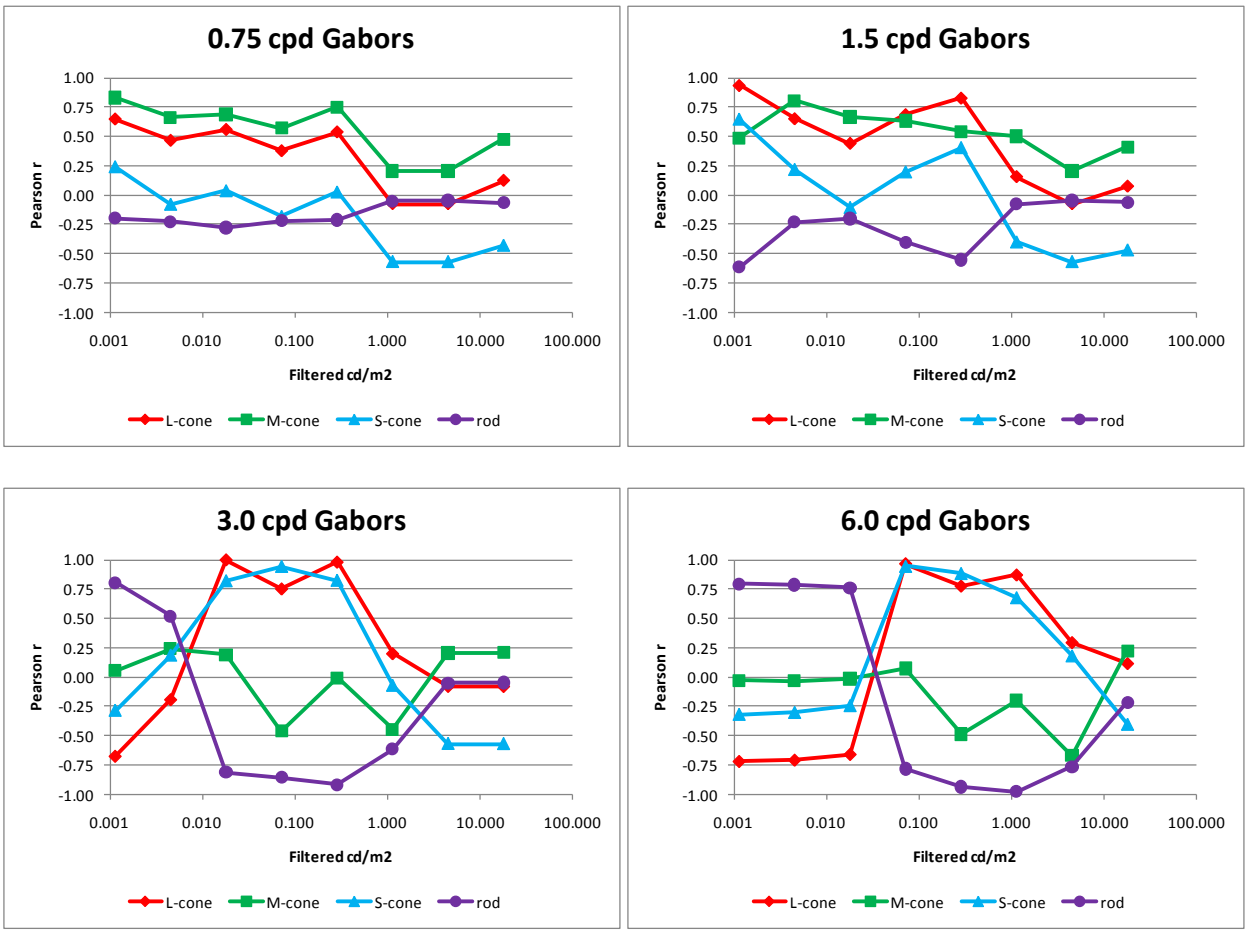

Figure 13 Correlations between photoreceptor projection and threshold u'v' distance in Experiment 3

5. EXP6: CHART CONTRAST SENSITIVITY AND ACUITY

5.1 Rationale

The phosphors of the Sony GDM-C520 CRT were shown in Figure 1. Compared to naturalistic visual stimuli, the phosphors can be very "spikey". That is certainly true of the red phosphor used in Experiments, 1, 2 & 4, and 3. For that monitor, the main spikes of the red phosphor are well past the peak of the l-cones sensitivity. That helps expand the monitor's gamut, but lowers photopic luminance. Experiment 6 was designed to test the generalizability of the previous results to broad band stimuli.

5.2 Method

5.2.1 Participants

One of the original male recruits failed the color screening and was replaced. Of the 12 participants for Experiment 6, there were six male and six female participants with a mean age of 20.9 years (18- 39).

5.2.2 Design and Stimuli

Experiment 6 was a 3 charts (Functional Acuity Contrast Test, Bailey Lovie high contrast, & Bailey Lovie low contrast) X 6 illuminant levels (66.4, 33.2, 16.6, 8.3, 4.15, & 2.08 mLux) X 4 goggle filters (none, ND, high pass, and low pass) repeated-measures design.

The Functional Acuity Contrast Test (FACT) was developed by Ginsburg (1984)[22]. It contains five rows of eight sine wave gratings. The orientation of each grating is vertical, tilt clockwise, or tilt counterclockwise. Spatial frequency increases from the top row (A) to the bottom row (E) and contrast is reduced by 0.15 log units from the leftmost grating on each row to the next grating on that row. From row A to row E, the contrast of the leftmost grating is 14.3%, 10%, 8.3%, 12.5%, and 25% (contrast sensitivity= 7, 10, 12, 8, and 4). Normally the FACT is viewed from 10' under normal office illumination and the spatial frequencies of rows A to E are 1.5, 3, 6, 12, and 18 cpd. To study mesopic vision, the viewing distance was reduced to 5', so the spatial frequencies were 0.75, 1.5, 3, 6, and 9 cpd in this experiment. Letter acuity was measured with charts designed by Bailey & Lovie (1976)[23]. Each chart has 14 rows of 5 letters at the same contrast. Moving up one line increases letter size by a factor of 1.26 (0.1 log units). This makes it easy to compute logMAR, since each letter is the same log unit difference and viewing distance can be reduced for low vision tests. Under office lighting, the chart is typically viewed from 6 meters (20') and the range of logMARs is 0.8 to -0.5. For this study, the viewing distance was 5', so the logMAR range was 1.4 to 0.1. In addition to two high contrast Bailey Lovie charts (BLHi), there are also two low contrast (Weber 18% and Michelson 10%) Bailey Lovie charts (BLLo).

All of the charts were illuminated by a Hoffman Engineering Variable Night Sky Projector (LM-33-80A). When the Night Sky Projector was set to "Full Moon" with f-stop= 4.5, chart irradiance was 66.4 mLux as measured with a Hoffman Engineering ANV-410 Photometer

(Class A filtered). The five lower levels were produced by adding ND filters in 0.3 OD steps. There were four viewing conditions. Three Hoya glass filters were mounted in welder's goggles. All had about 25% photopic transmittance (O58 was a bit higher and LB 145 was a bit lower). One was ND (ND25), one was high-pass with 50% transmittance at 560 nm (O580), and one was mainly low-pass with 50% transmittance at 443 nm (LB145). Figure 14 shows the same photoreceptor and phosphor functions as Figure 1, but the transmittance spectra of the Hoya filters have been added. The percent transmittance of each of the Hoya goggle filters with respect to each photoreceptor is shown in Table 3

Table 3 Photoreceptor-specific transmittance of the Hoya filters

%transmittance	photopic	l-cone	m-cone	s-cone	rod
O58	33.69%	40.33%	19.97%	0.01%	2.92%
LB145	21.46%	20.77%	24.17%	48.03%	31.58%
ND25	27.43%	27.36%	27.35%	23.87%	26.58%

5.2.3 Procedure

Two researchers (wearing NVGs) tested each participant in a session lasting less than 3 hours. After showing the participant the chart under normal office illumination, the participant dark adapted for 30 minutes in a light proof lab with the Night Sky Projector illuminating the blank, white backing of the FACT. The illuminant conditions were run in order from the lightest to the darkest. Within each illuminant condition, the four goggle filter conditions were conducted. The first test was always the none condition (no goggle). The order of the three Hoya filters was counterbalanced. Within each goggle filter condition, the order was always BLHi, BLLo, and FACT. Since there were two BLHi charts and two BLLo charts, the chart pairs were alternated between conditions.

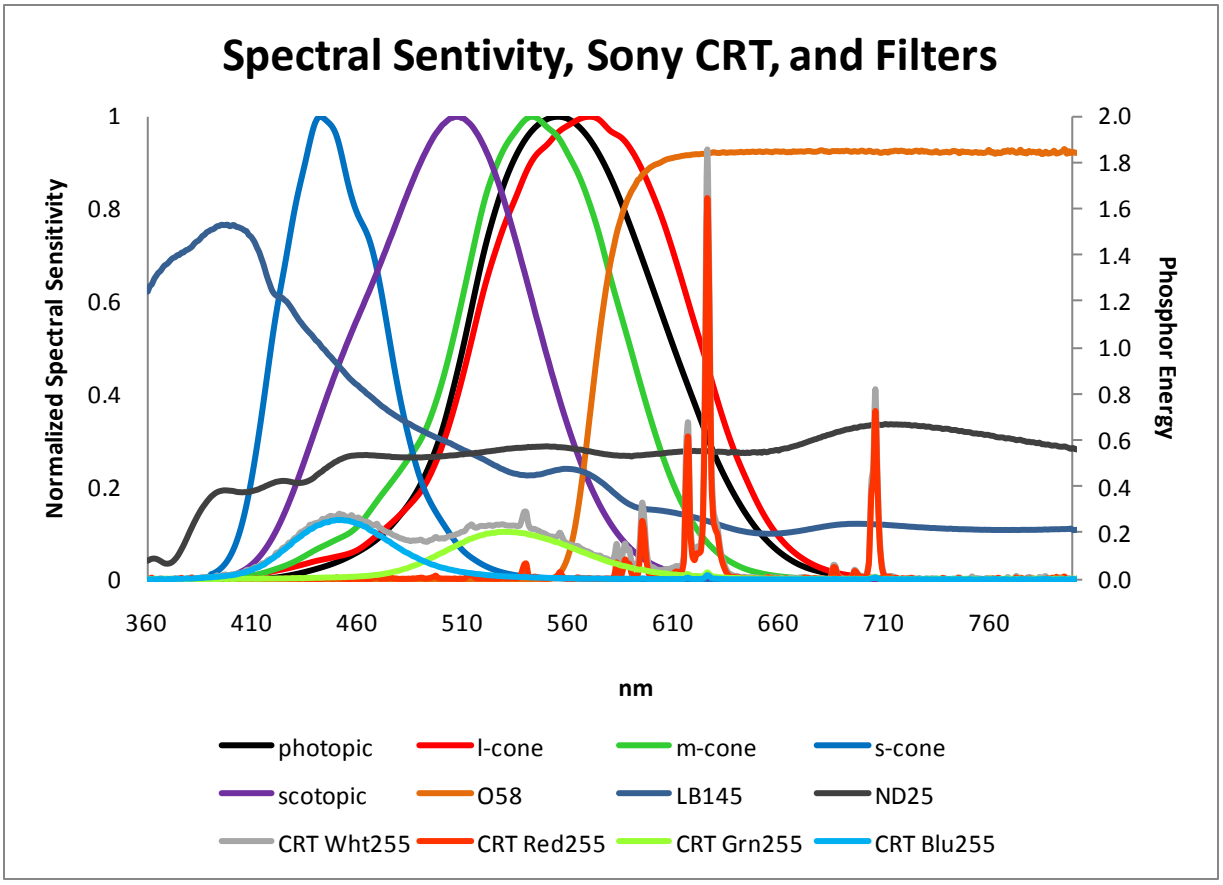

Figure 14 Transmittance spectra of the Hoya filters (O58, LB125, and ND25) compared to the photoreceptors and phosphors

5.3 Results

5.3.1 FACT

No participant ever saw a FACT grating from rows D and E (6 and 9 cpd). The contrast sensitivities for the lower spatial frequency gratings are shown in Figure 15. As expected, contrast sensitivity was low pass: contrast sensitivity decreased as spatial frequency increased. Contrast acuity through the ND25 filter was close to the contrast acuity in the None condition (no goggle) at 25% of the irradiance. This suggests that the no goggle control was satisfactory compared to a clear glass Hoya filter. The no goggle control was chosen because wearing the welder's goggles can get uncomfortable over time. No one ever saw a grating through the O58 filter. Based on Table 3, clearly l-cones were not being used. It also seems unlikely that m-cones were being used. The 19.97% m-cone transmittance through the O58 filter should have been detectable at the 66.4 mLux irradiance of the 0.75 cpd gratings. It is most likely that vision was scotopic for the FACT, because contrast sensitivity is generally similar for the ND25 and LB145 filters. Rod transmittance is similar through the two filters, but s-cone transmittance is almost twice as high through the LB145 filter as through the ND25 filter.

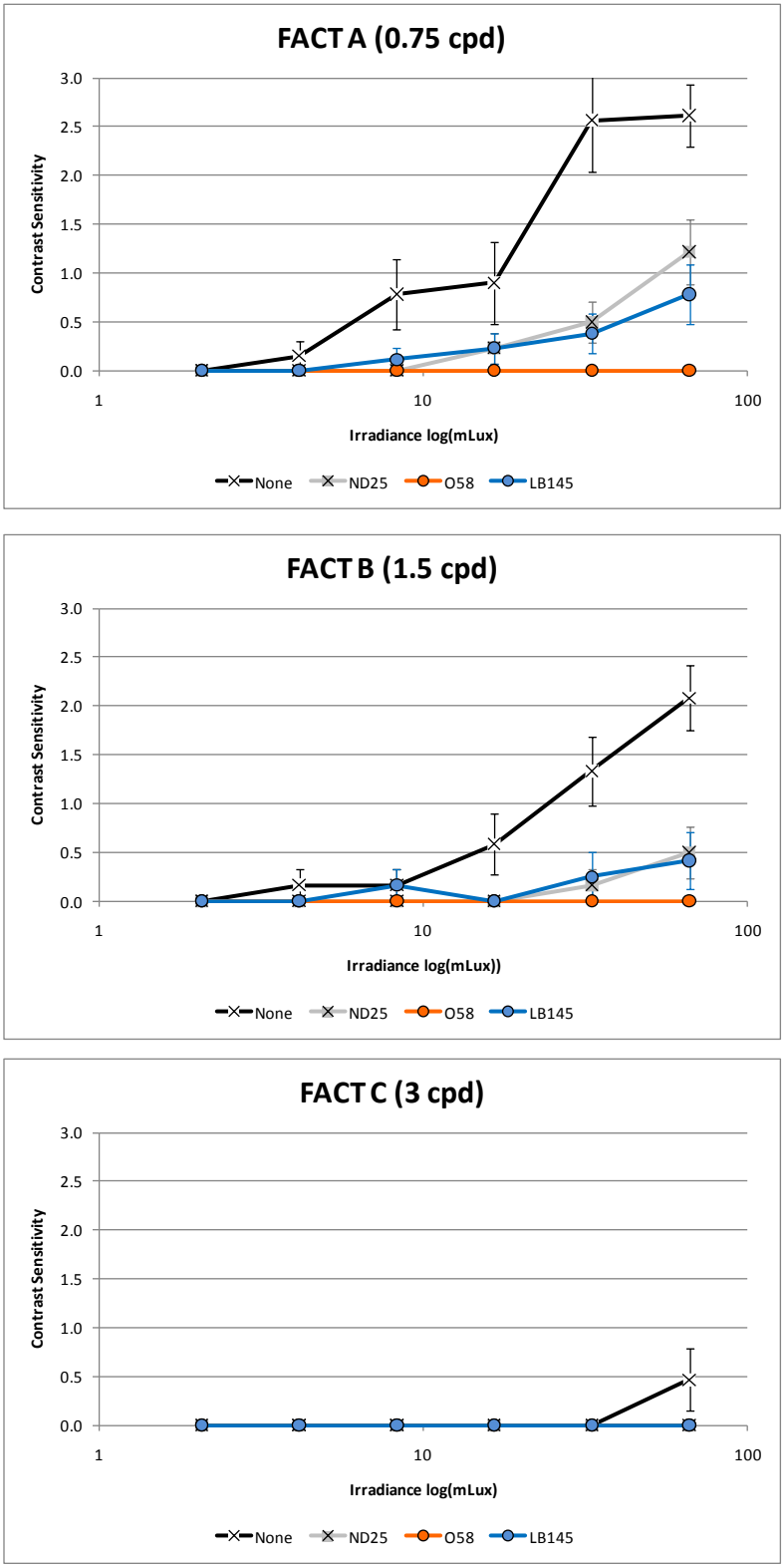

Figure 15 Contrast sensitivity for the FACT charts in Experiment 6

5.3.2 Bailey Lovie Contrast Acuity

Acuity for the Bailey Lovie high and low contrast charts are shown in Figure 16. As was found in FACT contrast sensitivity, Bailey Lovie acuity through the ND25 and LB145 were similar to each other and comparable to the no goggle acuity at one quarter irradiance. In general, acuity was much worse (higher logMAR) through the O58 Hoya filter. Notably, only one observer was able to read one letter on the BLLo chart at the highest irradiance. On the other hand, acuity for the BLHi chart at the highest irradiance was equivalent between the O58 and the ND25 & LB145 filters. That suggests m-cone input in that condition. Table 3 shows the m-cone transmittances to be similar for the three Hoya filters. At lower irradiances, O58 acuity drops off rapidly. Low O58 acuity with comparable ND25 and LB145 acuity indicates a shift to rod input.

5.4 Conclusions

In general, the Experiment 6 data indicate scotopic processing. The exception is m-cone input for acuity with the BLHi chart at the highest irradiance. In that condition logMAR= 1. That means that the stroke width is 10 minutes of arc (Snellen Equivalent= 200) or cpd= 0.33. The m-cone input was robust in contrast sensitivity for the larger letters (stroke width of 10 and 20 minutes of arc) at low filtered luminances in Experiments 2 & 4. The 3 cpd letters in BLHi have a lower spatial frequency than the lowest FACT spatial frequency grating or the lowest gabor spatial frequency tested in Experiment 3 (0.75 cpd in both cases).

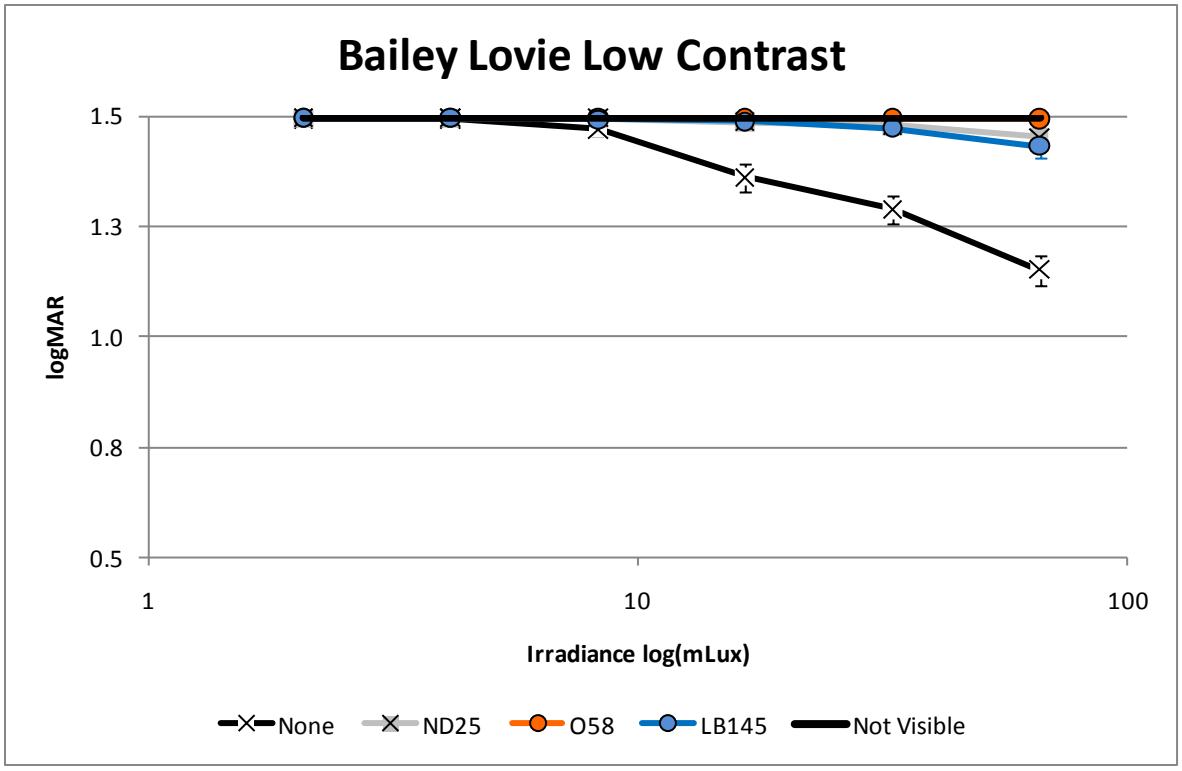

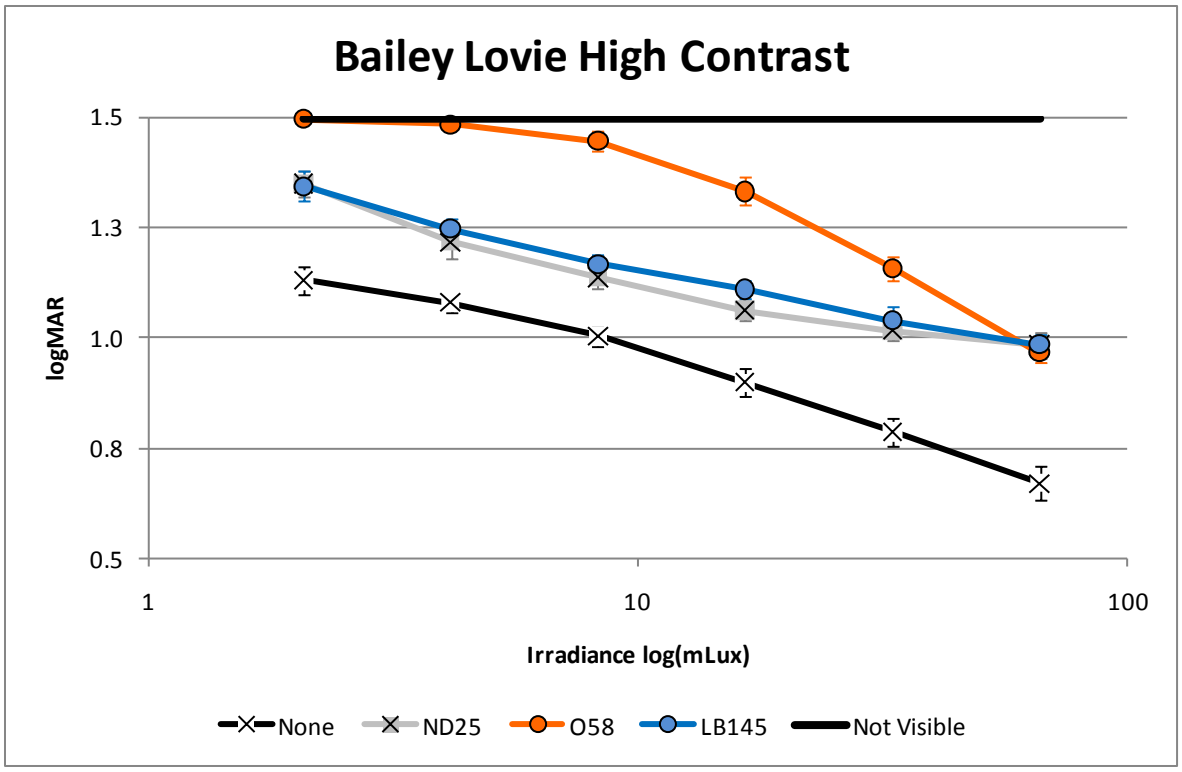

Figure 16 Contrast acuity for the Bailey Lovie charts in Experiment 6

6. EXP7: COLOR NAMING FOR THE MACBETH COLORCHECKER

6.1 Rationale

Even within the photopic range, color zones shrink as luminance is reduced[24]. Color perception must fade as vision shifts from cones to rods across the mesopic range. Experiment 7 investigated color vision for the Macbeth ColorChecker using the same Night Sky Projector used in Experiment 5.

6.2 Method

6.2.1 Participants

One of the original male recruits failed the color screening and was replaced. Of the 12 participants for Experiment 7, there were six male and six female participants with a mean age of 19.6 years (18- 22).

6.2.2 Design and Stimuli

Experiment 7 was a 24 stimuli (the Macbeth ColorChecker has 24 chips) X 2 backgrounds (white or black) X 2 reference conditions (absent or present) X 3 goggle filter conditions (none, ND25, or chromatic) X 2 chromatic filter conditions (O58 or LB145) mixed design. Six participants used the O58 chromatic filter and the other six used the LB145 chromatic filter.

The 24 Macbeth ColorChecker chips are designed to mimic naturalistic stimuli (e,g,; skin, foliage, sky) to help photographers adjust chromaticity and exposure level. Their chromaticities (included with the ColorChecker and based on Illuminant C) are plotted in Figure 17. For half of the trials, the test chip was velcroed onto a white foam board and for the other half the test chip was velcroed onto a black foam board. Within each background color, two boards were constructed. In one case, the velcro patch was in isolation (no references). In the other case, all 24 of the ColorChecker chips were mounted in two rows and columns surrounding the test chip to serve as references (references present). Viewed from a distance of 46.5 inches, each square chip subtended 2° on a side.

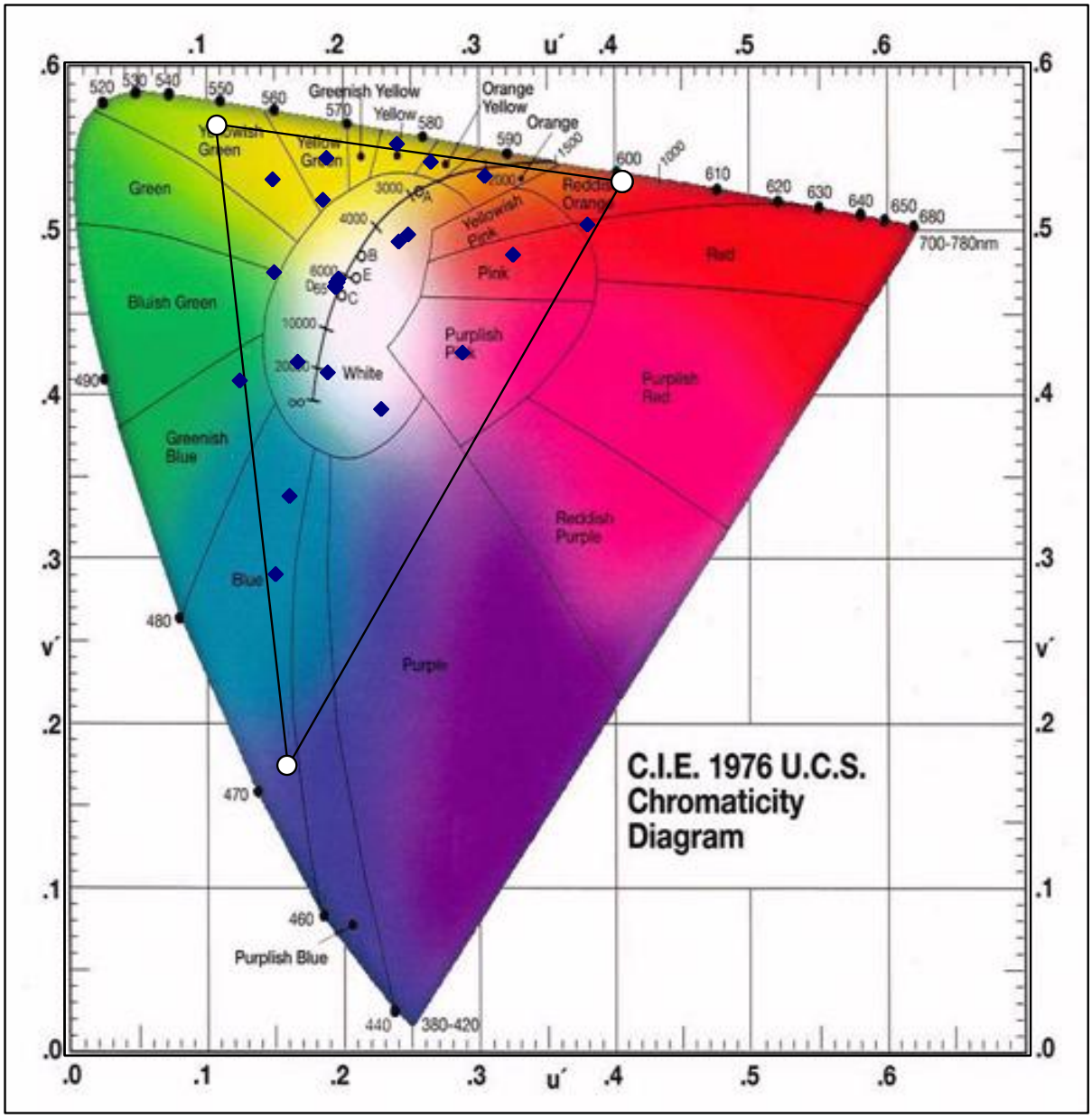

Figure 17 The 24 Macbeth ColorChecker stimuli used in Experiment 7

6.2.3 Procedure

Two experimenters wearing NVGs tested each participant in a session lasting less than 3 hours. One experimenter controlled stimulus presentation and the other recorded the reported color name. As in Experiment 6, the participant was shown all of the stimuli under normal office lighting prior to a 30 minute dark adaptation period with the same Night Sky Projector used in Experiment 6. In this experiment, participants also practiced color naming prior to adaptation. The goal was to place minimal, but systematic constraints on the color names the participant could use. The scheme was based on an extension of the Level 2 Universal Color Language (USL) proposed by Kelly & Judd (1976)[25]. The 29 Level 2 color names are based on the 13 Level 1 color names. Those 13 Level 1 color names include the 11 Stage VII basic color names proposed by Berlin & Kay (1969)[26]: red, orange, yellow, green, blue, purple, pink, brown, black, white, and grey. The additional Level 1 colors included were yellow green and olive. The 29 Level 2 color names included directional intermediate colors (e.g.; greenish blue and bluish green). Kelly & Judd allowed a number of modifiers to the 29 Level 2 color names to generate the 267 color names in their Level 3. Only the "light", "dark", and "grayish" modifiers were allowed in the Experiment 7 color naming.

All trials were conducted at the "Full Moon" with f-stop= 4.5 setting of the Night Sky Projector (66.4 mLux). All participants first did the no goggle condition. That was followed by the ND25 goggle condition and then whichever chromatic goggle was assigned (either O58 or LB145). Within goggle filter condition, the order of background and reference conditions was always white with references present, white with no references, black with no references, and black with references. The order of goggle filters and background helped maintain adaptation, but the order of background and reference conditions conforms to a digram-balanced Latin Square. All 24 ColorChecker chips were named within each of the goggle X background X reference conditions. The 24 stimuli were divided into four sets of 6 stimuli. Each set sampled across the u'v' space. A rotating scheme was implemented that made it possible for one of the experimenters to present the chips in a timely manner while counterbalancing the order of the four sets and the chips within each set.

6.3 Results

The color names given for each chip were tabulated across participants (across 12 participants for the none & ND25 goggle conditions and across 6 participants for the O58 & LB145 goggle conditions). In order to summarize those tabulations, a subset of color names was selected: nine chromatic names (red, orange, yellow, green, blue green, blue, purple, pink, and brown) and three achromatic names (white, grey, and black). The relevant name was assigned if there was agreement across at least 9 of the 12 participants in the none & ND25 goggle conditions or across at 5 of the 6 participants in the O58 & LB145 goggle conditions. Adjacent names were combined (e.g.; a red name and a blue name were treated as two purples; a green name and a blue name were treated as two blue greens), but opponent names produced a cancellation (e.g.; if several people named a chip red, then a green response was treated as achromatic). If there was moderate consensus about a color name (5-8 out 12 participants or 3-4 out of 6 participants),

then the relevant chromatic name was assigned the "desaturated" modifier. Chips lacking a consensual chromatic name (≤ 4 out of 12 or ≤ 2 out of 6) were assigned an achromatic name.

The loci for the full chromatic names were usually evaluated as the location on the monitor's gamut based on the centroid u'v' coordinates. The two exceptions were pink (less saturated than red) and brown (a slightly desaturated yellow orange). All achromatic names (white, grey, and black) were set to Illuminant D (0.198, 0.468). The desaturated loci were the midpoint between each full chromatic locus and Illuminant D. Those loci are shown in Figure 18: white diamonds represent full chromatic color appearances, grey circles represent desaturated color appearances, and the Ж is achromatic (Illuminant D). Fairchild[27] graphically shows shifts in color appearance with arrows in the color space. The tail is the source locus in space and the arrow tip is the appearance. That convention is used in Figures 19- 21. Each figure shows a goggle condition (None, ND25, O58, and LB145). The four graphs within each figure show how the appearance of the stimulus colors shifted within each of the four background X reference combinations.

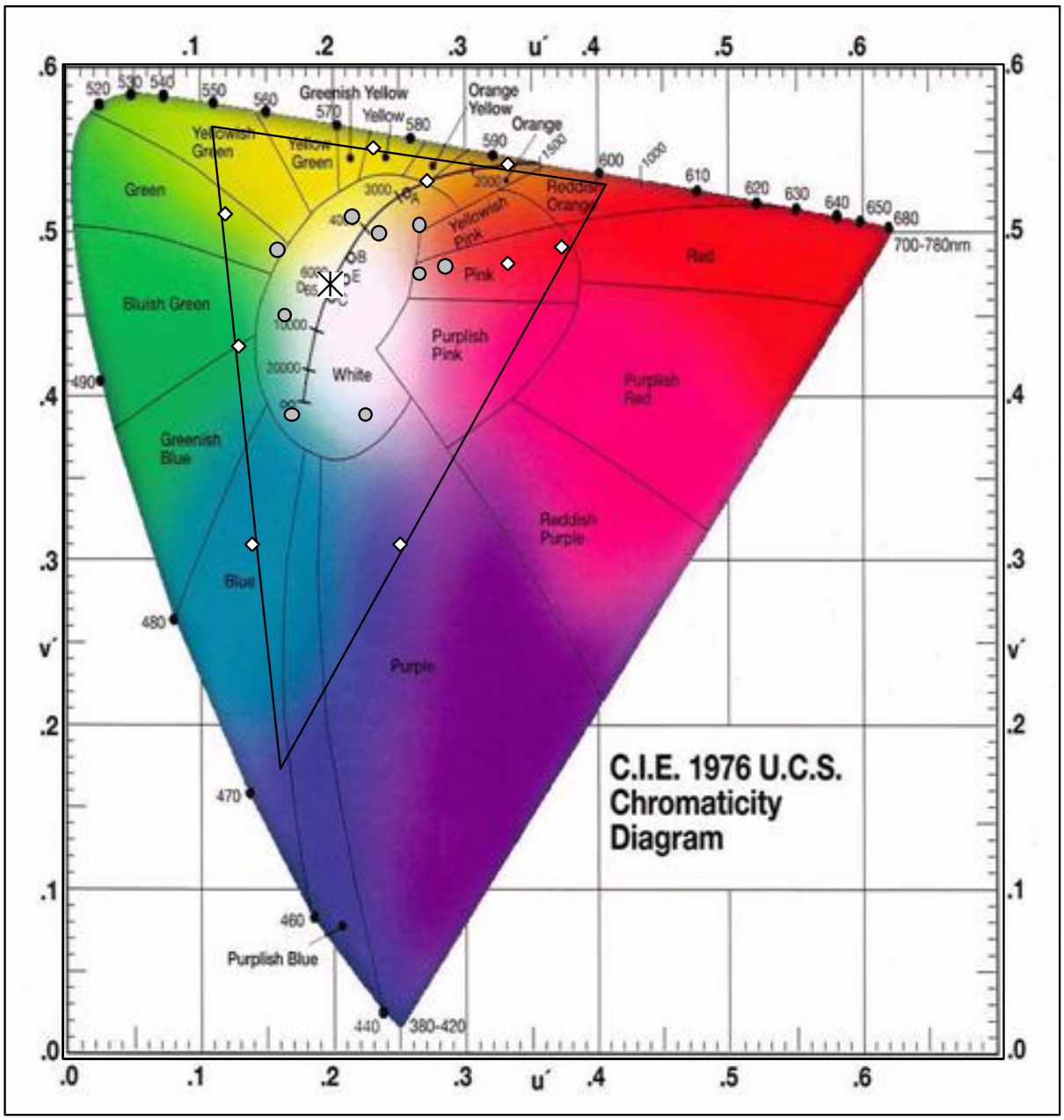

Figure 18 The loci for the color appearance names in u'v' space

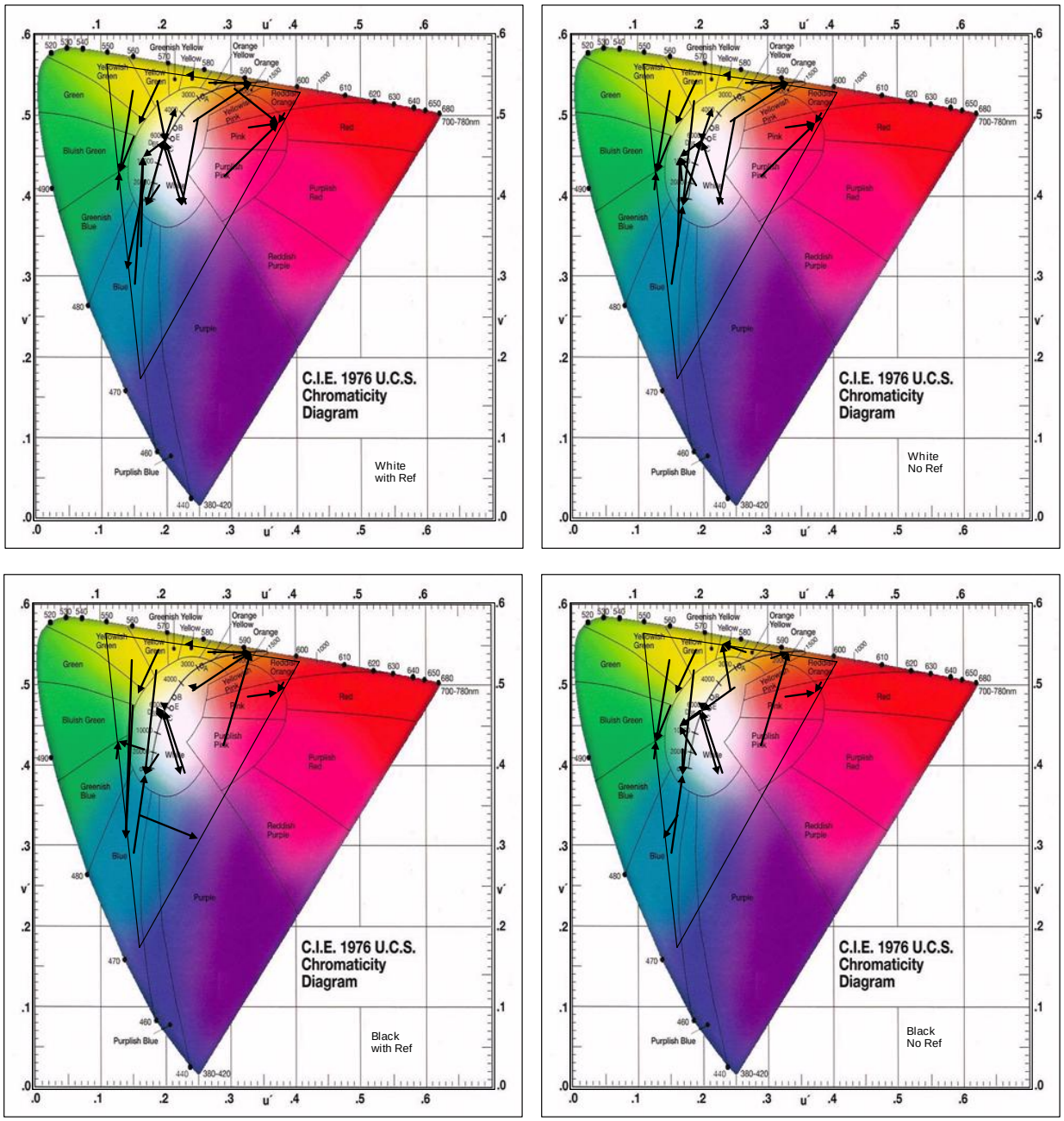

Figure 19 The color appearance shifts in Experiment 7 for the no goggle condition

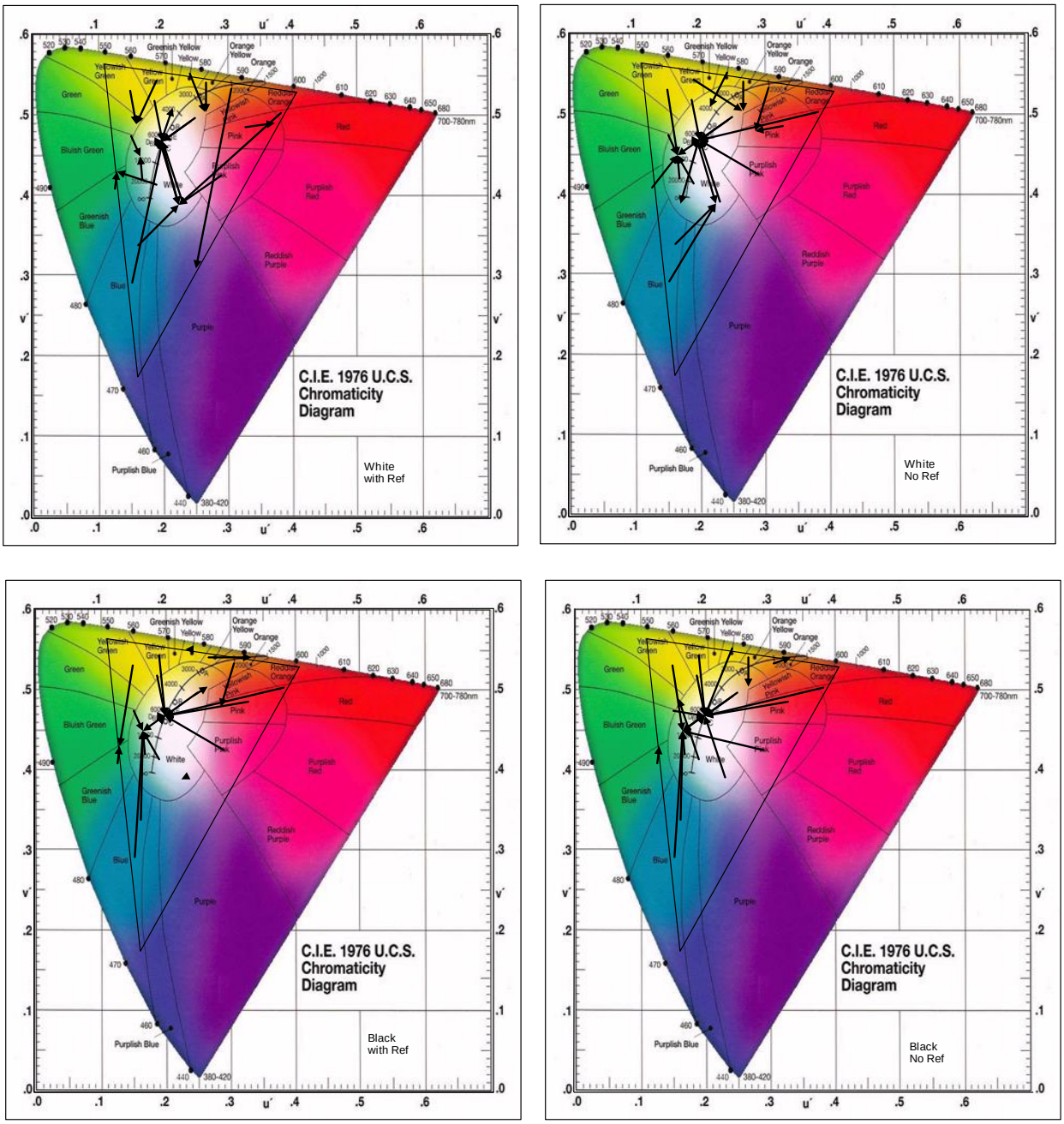

Figure 20 The color appearance shifts in Experiment 7 for the ND25 goggle condition

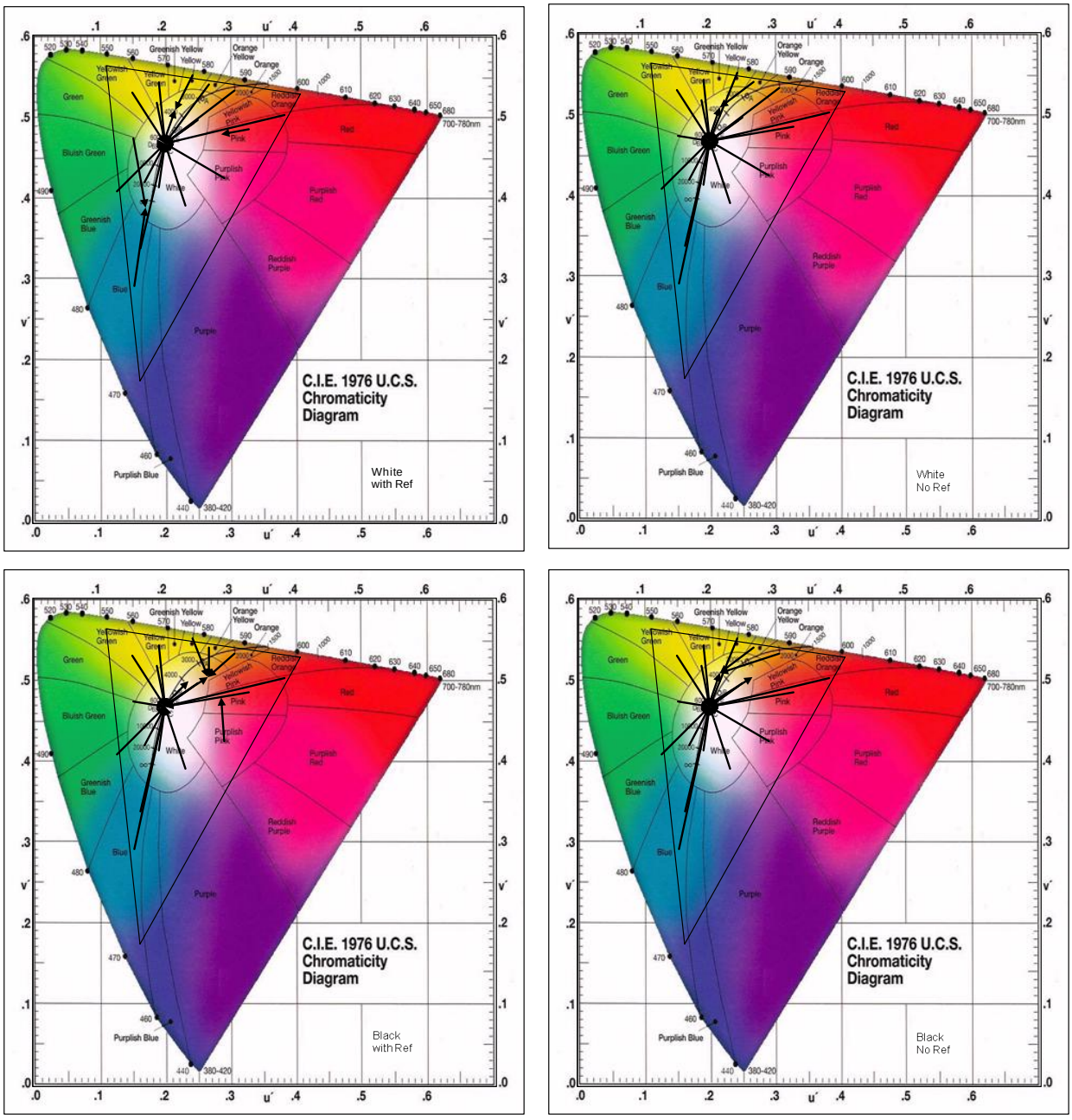

Figure 21 The color appearance shifts in Experiment 7 for the O58 goggle condition

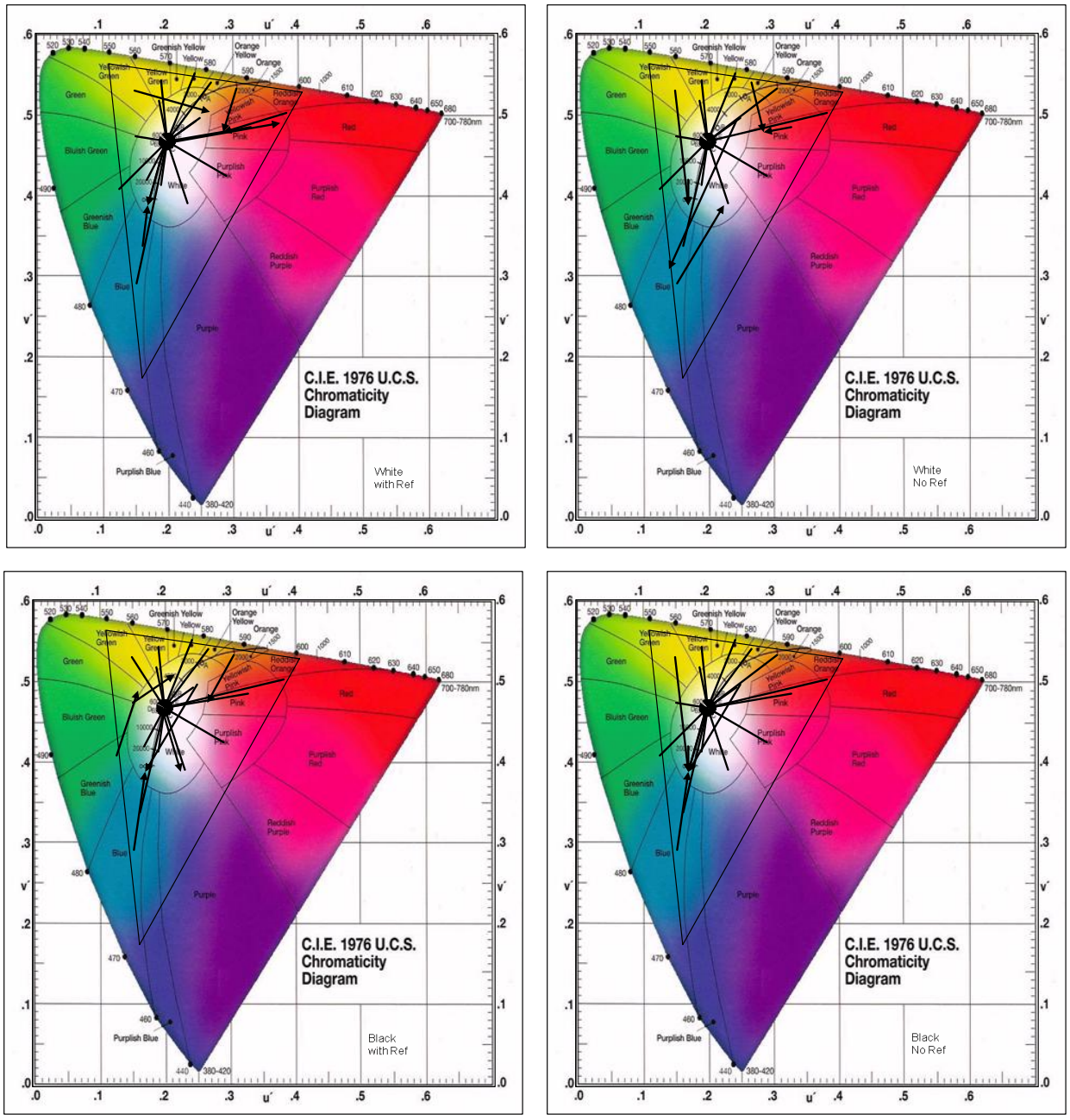

Figure 22 The color appearance shifts in Experiment 7 for the LB145 goggle condition

In the no goggle condition (Figure 19), most stimuli show a loss of saturation; but there appears to be loss of yellow appearance with systematic shifts either toward red or toward cyan or blue. With the ND25 goggles (Figure 20), there is greater desaturation and the shifts are generally only toward cyan and blue (most shifts are away from red). There is almost total desaturation with the O58 and LB145 goggles, but there were some very isolated shifts with the LB145 goggles. The overall results of the strong goggle effects are summarized in Table 4.

Table 4 Mean chromaticity of color appearances as a function of goggle in Experiment 7

	None	ND25	O58	LB145
Chromatic	11.00	2.50	0.00	0.50
Desaturated	8.50	11.25	4.25	5.75
Achromatic	4.50	10.25	19.75	17.75

While the effect is much smaller, Table 5 suggests that the reference colors may help maintain some chromaticity of color appearances in the mesopic range.

Table 5 Mean chromaticity of color appearances as a function of background and references in Experiment 7

	White Ref	White No Ref	Black Ref	Black No Ref
Chromatic	4.00	2.75	4.00	3.25
Desaturated	8.00	8.00	6.75	7.00
Achromatic	12.00	13.25	13.25	13.75

6.4 Conclusions

Even under full moon illumination, most of the Macbeth ColorChecker chips maintained fair chromaticity with shifts toward cyan, blue, and red. Reducing the illuminant by 25% (ND25) increased desaturation and the shift in red appearance was further reduced. Both of the achromatic filters reduced the illuminant about 25%, but their spectral selectivity almost eliminated any appearance of chromaticity. They were only a very few exceptions with the LB145 goggle. Again, l-cones seem no longer operational and s-cones may have some small effect.

7. EXP5: COLOR NAMING ON A CRT

7.1 Rationale

While Experiment 7 documented the reduction in chromaticity in the mesopic range, shifts in the appearance of specific colors was much less clear. They may be clearer with the "spikey" spectral stimuli presented on the CRT. Also, it may help to study changes in color zones. That required more stimuli than the 24 in the Macbeth ColorChecker. In addition, they must be distributed across the CRT's gamut.

7.2 Method

7.2.1 Participants

All 24 participants for Experiment 5 passed the screening and were included for data analysis. There were 16 male and eight female participants with a mean age of 20.3 years (18- 29).

7.2.2 Design and Stimuli

Experiment 5 was a 48 stimuli (augmented Macbeth ColorChecker stimuli presented on the CRT) X 8 luminance levels (filtered by the gels) X 3 goggles (None, ND25, and a chromatic goggle) X 2 (O58 or LB145 chromatic goggle) mixed design. Twelve of the participants used the O58 goggle and 12 used the LB145 goggle. All of the other independent variables were repeated measures. It was necessary to split the trials across two 2-hour sessions scheduled two days apart.

All of the stimuli were presented on the same Sony GDM-C520 CRT used in Experiments 1- 4 and the same eight gels were used to reduce overall luminance (transmittance from 97% to 0.006%). The goal was to have all of the stimuli have Y= 18 cd/m², but that was not possible. A compromise was made with the bluest stimulus: its chromaticity was reduced by adding enough red and green phosphor to set its Y= 10 cd/m². Overall the median luminance was Y= 18.2 (mean= 17.9 cd/m²). In general, the luminance range across the 8 gels was from 17.5 cd/m² to 0.0011 cd/m². On the other hand, there was some variation between stimuli and it is more accurate to refer to the gels. There were 16 stimuli created to match Macbeth ColorChecker stimuli. There were four anchors: the three vertices of the gamut (except for blue) and Illuminant C. The other 28 stimuli were chosen to evenly sample across the gamut in CIE u'v' space. The stimuli are shown in Figure 23.

Each stimulus was the same size as the chips in Experiment 7 and the viewing distance was again 46.5 inches. Consequently each stimulus subtended 2° of visual angle. Each "chip" was surrounded by a 1/16 inch black border (similar to Macbeth ColorChecker) in a PowerPoint slide with a background set to Illuminant C at the same luminance as the darkest (blue) stimulus: Yxy= 10, 0.310. 0.312. Each slide also contained four references of the same size as and diagonally offset from the stimulus square. The top and lower left references were the gamut colors at Y= 10 cd/m². The lower right reference was a 3X3 matrix. The top row was Illuminant C, but lighter than the background (Y=15 cd/m²). The bottom row was Illuminant C, but darker than the background (Y= 5 cd/m²). The middle row repeated the gamut colors in thirds (GBR left to right).

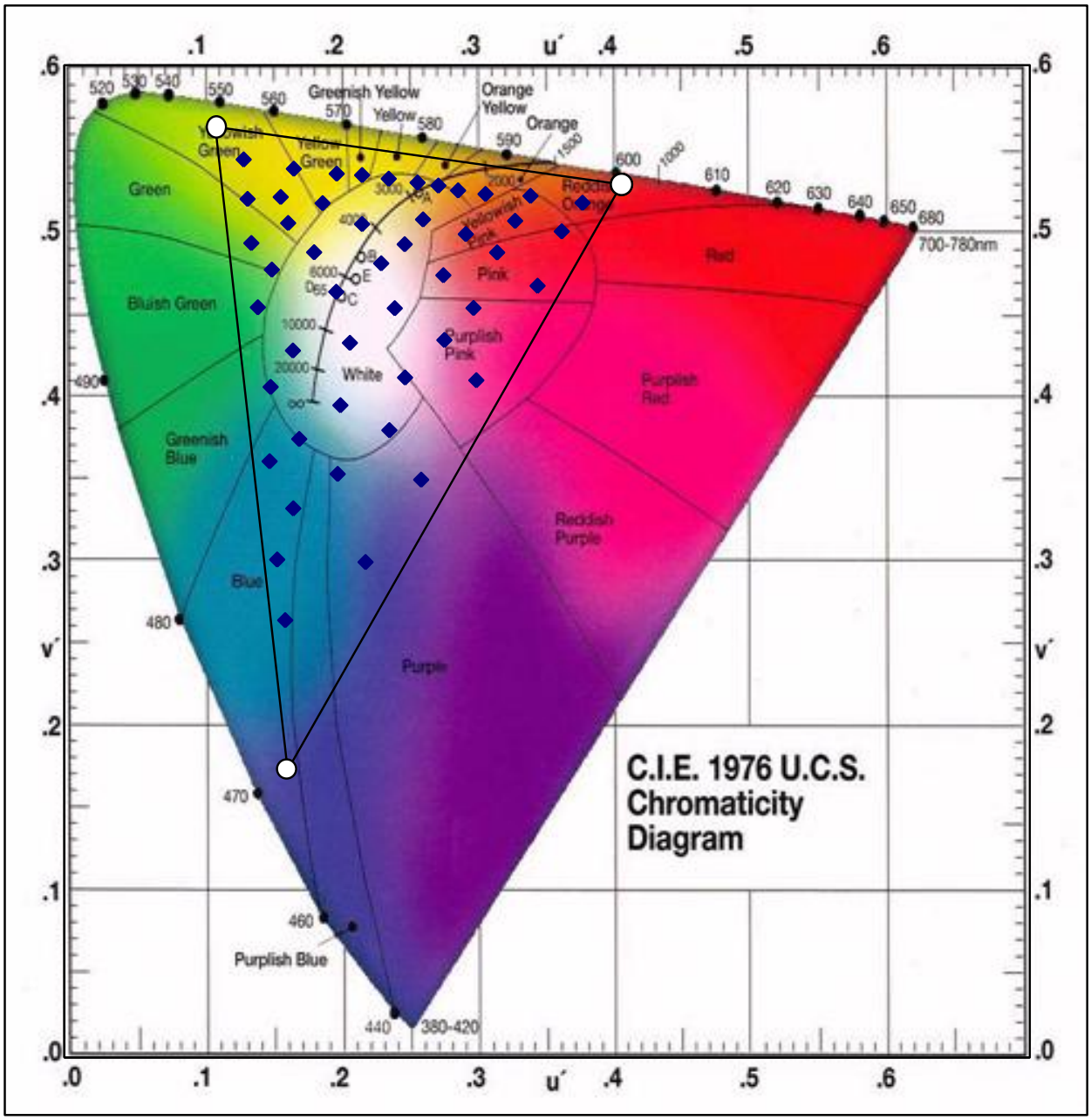

Figure 23 The stimuli presented in Experiment 5

7.2.3 Procedure

Two researchers wearing NVGs at the lower luminances conducted the experiment with each participant. Participants were randomly assigned to the O58 and LB145 condition for both sessions. Four sets of 12 stimuli were created that each systematically sampled across the gamut. Within each session, the participant dark adapted for 15 minutes by playing the video game and then went through the eight gets from lightest to darkest. There was a PPT slide show for the 72 trials in each gel. The first 24 trials were run with no goggle (two set of 12) and the last 48 were either with the ND 25 or that participant's chromatic goggle (all four sets of 12). The ND25 and chromatic goggle alternated between gels. The order of sets alternated between blocks and their order was counterbalanced. On the second day, the other two sets were run in the no goggle condition and the other of the chromatic and ND25 goggle was tested in each gel. The same color naming conventions were used as in Experiment 7.

7.3 Results

The color names were tabulated across all 24 participants in the none and ND25 goggle conditions and across all 12 participants in each of the O58 and LB145 goggle conditions. Ignoring sessions, a summary of all color names assigned by at least two participants was created for all 1152 stimulus combinations (48 X 8 X 3). This summary was used to compute radial color appearance space. Hue angle was based on defining red, yellow, green, and blue to be 0°, 90°, 180°, and 270°. Orange, yellow green, blue green, and purple were interposed at 45° intervals. Radial distance was based on chromaticity similar to Munsell's descriptors: Vivid / Brilliant was defined as 60. Light /Dark modifiers were defined as 40, grayish modifiers were defined as 20, and achromatic was defined as 0. The mean across participants of the cross-products of the number of color names and hue angle definitions produced that stimulus's hue angle. The mean across participants of the cross-products of the number of color descriptors and the chromaticity definitions produced that stimulus's chromaticity. As in Experiment 7, a response that was the opposite of (180° from) a common response was recoded as achromatic. While singleton responses were uncommon across the 24 participants in the none and ND goggle conditions, they were not uncommon across the 12 participants in the O58 and LB 145 goggle conditions. Such singletons were ignored in terms of hue angle, but each added a half of an achromatic response in terms of computing chromaticities. Pairs of color appearance coordinates were used to define color zones.

All trials in a given gel and goggle condition were first sorted by hue angle and then broken into bins for the eight color categories defined above. Then each bin was sorted by chromaticity. Pairs of points that crossed a color name border (were in adjacent hue angle bins) and that shared a similar chromaticity were chosen. Their midpoint was chosen as lying on a color name border. It's coordinates in the color appearance space was then mapped back onto the u'v' space. A best-fitting line through the central set of those points and originating at Illuminant C was computed. It should be noted that, based on different set s of pairs, there were often multiple radii for the same border. The central and best-fitting radius was chosen. Secondly, the coordinates were sorted by chromaticity and split into bins that straddled a 10, a 30, and a 50 chromaticity border. Points within each bin were then sorted by hue angle. Pairs of points that straddled a chromaticity border and were close to each other in hue angle were chosen. Their midpoint was chosen as a point on that chromaticity contour in the color appearance space. A

polynomial fit of those contour points was then computed in MATLAB. The resulting equation was then mapped back onto the u'v' space. The process was successful for all of the no goggle data except that no Chroma 50 contour could be computed for Gel 8. For the ND25 data, Chroma 50 contours could not be computed for Gels 7 or 8 and a Chroma 30 contour could not be computed for Gel 8. Consistent with the Experiment 7 data, there were too few points to construct many chroma contours with the O58 and LB145 data.

For the no goggle data, the color appearance zones mapped into u'v' space are shown in Figures 24 and 25. The hue borders remain quite stable up to Gel 4 where the green borders seem to split. Two of the green borders reverse position in Gel 5 and the chromaticity borders expand (chromaticity decreases). Performance for both borders and chromaticity is remarkably high for Gel 6 before declining gain for Gel 7. For Gel 8, several best fit hue lines switch positions and chromaticity is almost nonexistent (there is no Chroma 50 contour, the Chroma 30 contour barely fits in u'v' space, and the Chroma 10 contour almost fills the gamut).

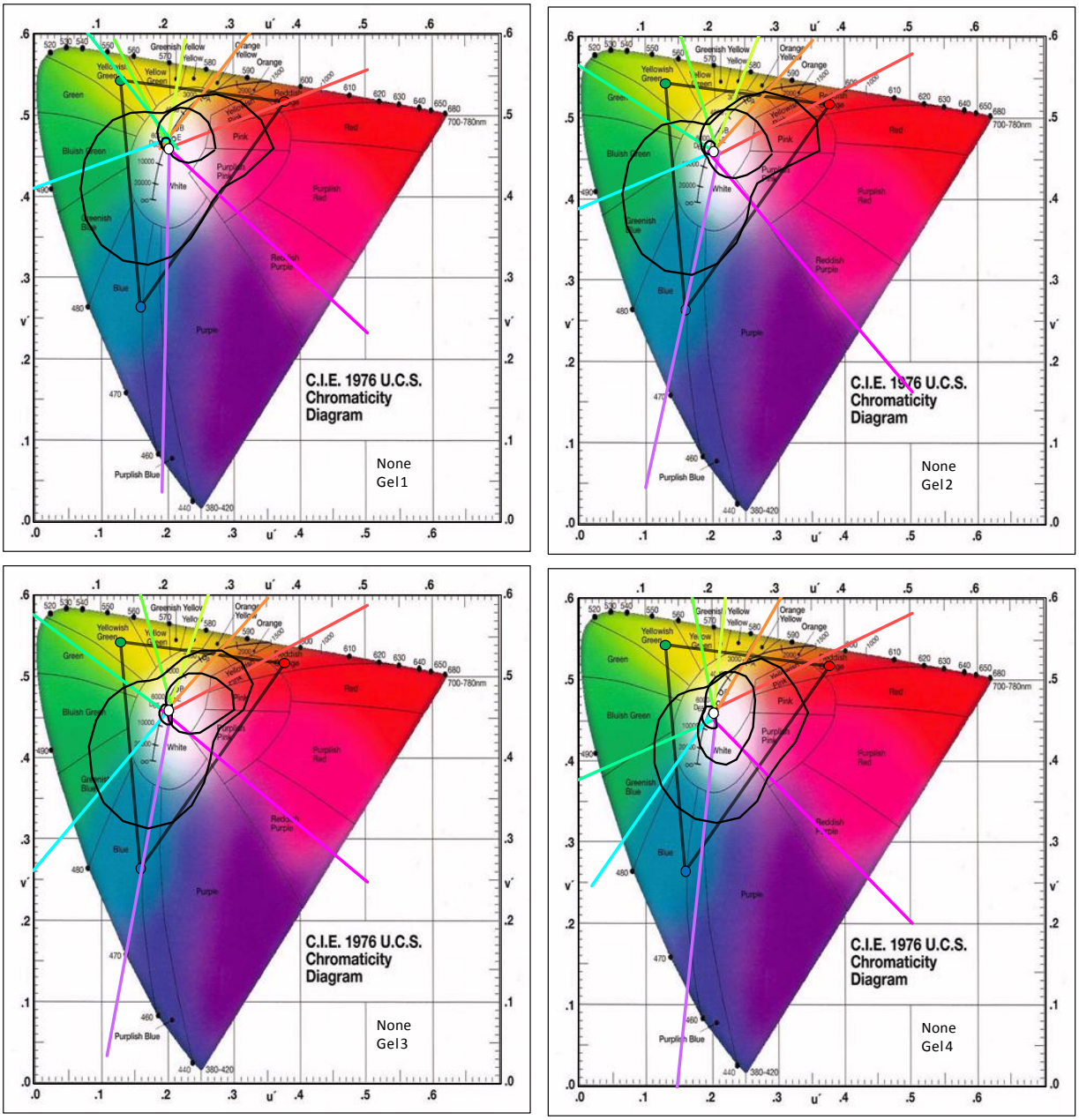

Figure 24 Color appearance zones for Gels 1- 4 with no goggle in Experiment 5

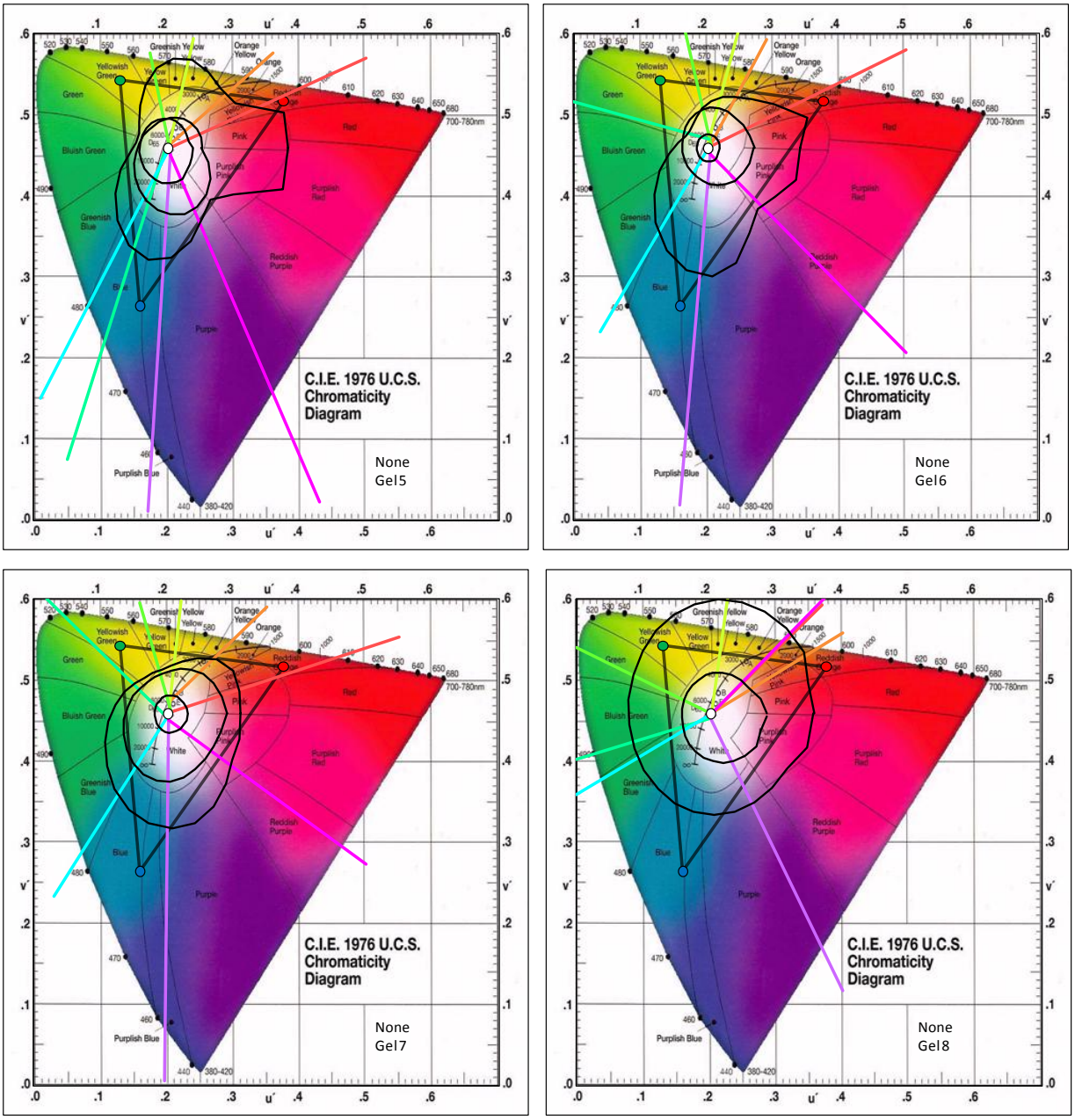

Figure 25 Color appearance zones for Gels 5- 8 with no goggle in Experiment 5

The ND25 data are shown in Figures 26 and 27. The green blue border starts to shift in Gel 2 and the green yellow border starts to shift in Gel 4. These are about the same luminance as Gels 3 and 5 in the no goggle condition. By Gel 6 (about the same luminance as Gel 7 in the no goggle condition) hue categories start to be lost: yellow in Gel 6, Purple in Gel 7, and Yellow, Yellow Green, & Purple in Gel 8. If a hue category is lost, the borders on each side are also lost. As with the no goggle data, chromaticity is also lost as luminance decreases in the ND goggle data. The Chroma 10 contour is expanded in Gel 3. By Gel 7 (about the same luminance as Gel 8 in the no goggle condition), there is no Chroma 50 contour and the Chroma 10 contour fills much of the gamut. There are no Chroma 50 or Chroma 30 contours for Gel 8.

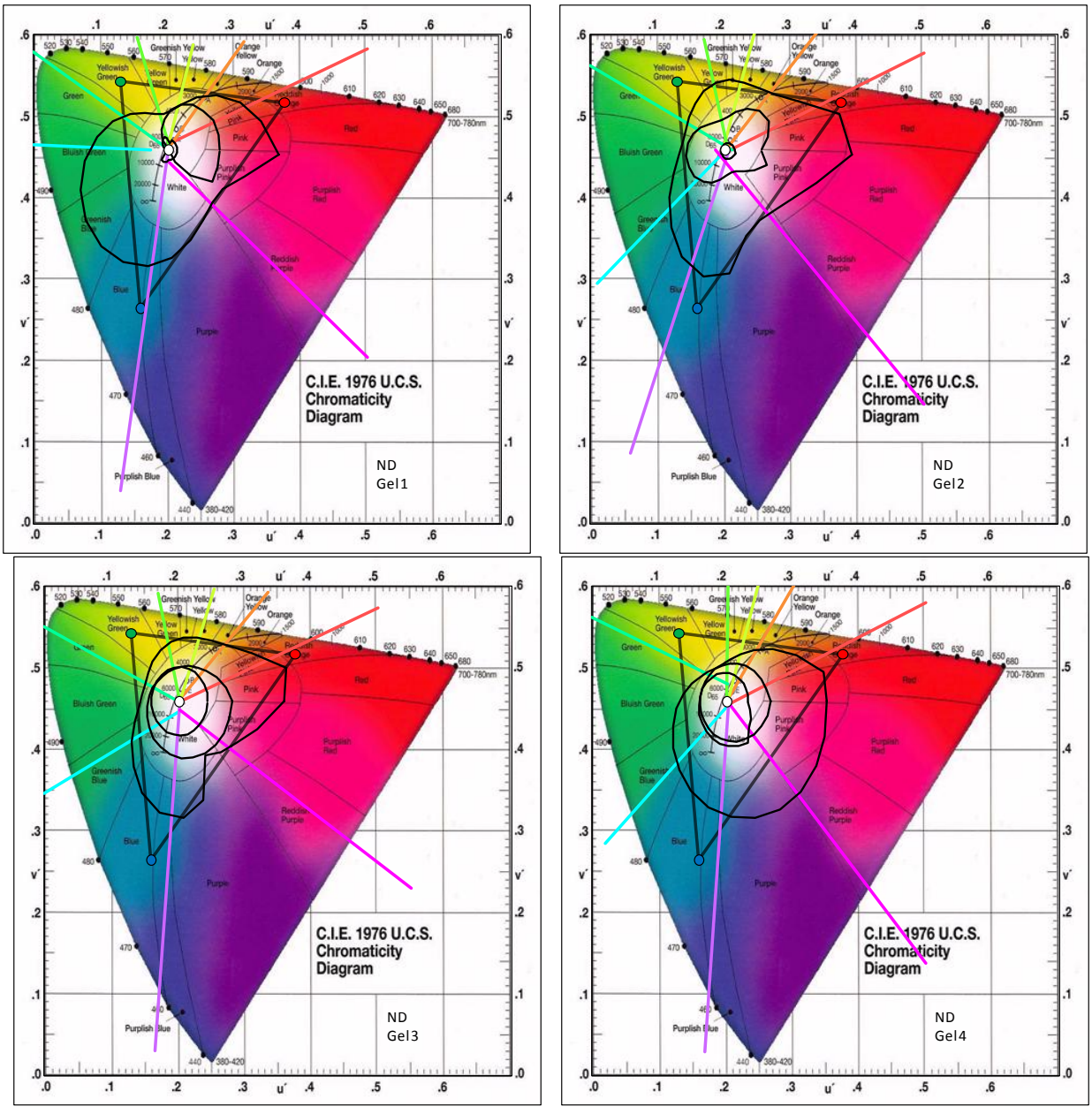

Figure 26 Color appearance zones for Gels 1- 4 with the ND25 goggle in Experiment 5

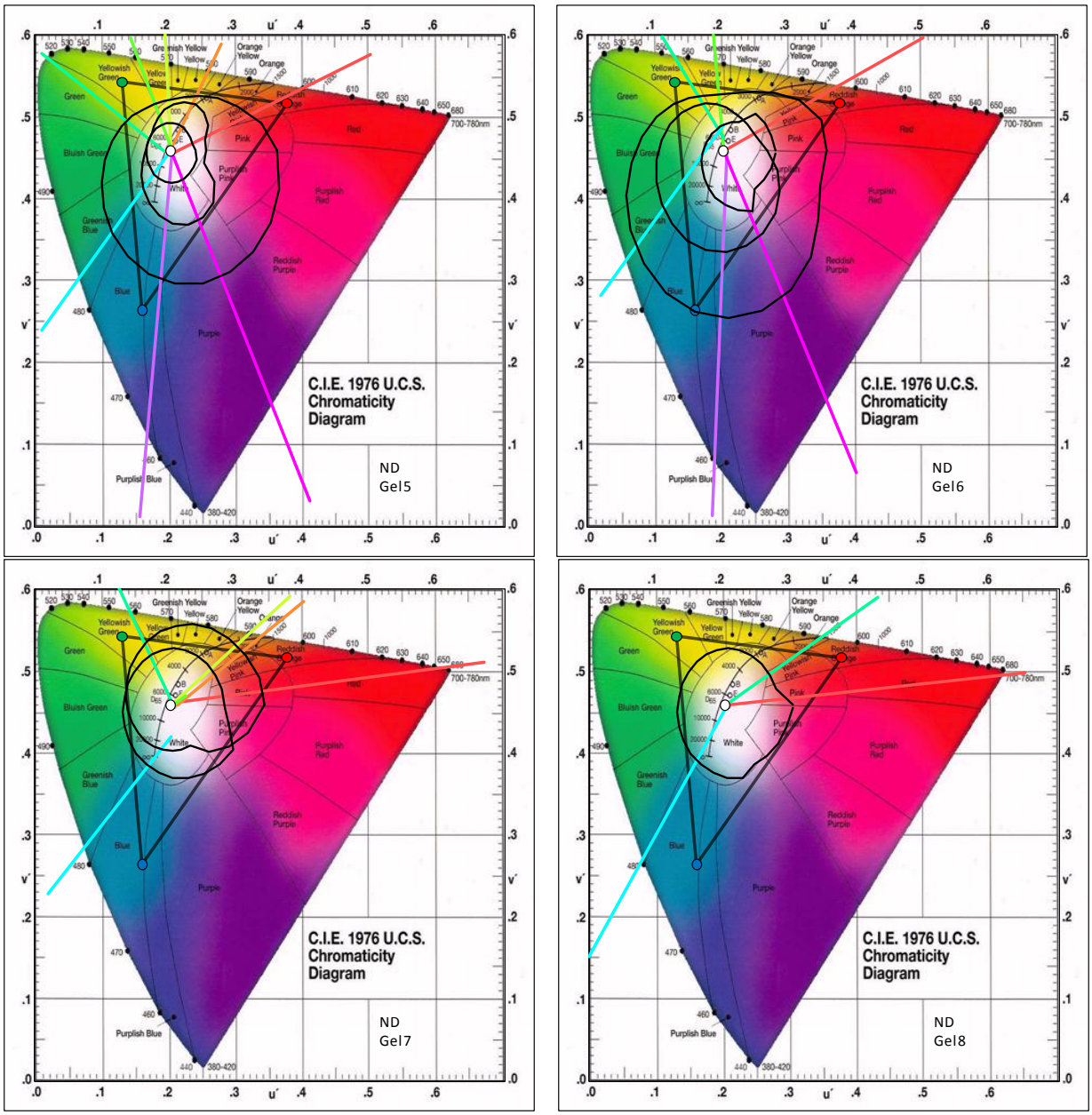

Figure 27 Color appearance zones for Gels 5- 8 with the ND25 goggle in Experiment 5

The data for Gels 1 and 2 with the O58 goggle are shown in Figure 28. There are no blue or purple color zones (nor their borders) for Gel1. There are no blue green or purple color zones for Gel 2. Performance did not improve as luminance was further reduced. As with Experiment 7, color naming performance is much worse with the O58 goggle than with the ND25 goggle even comparing similar overall transmittance. The difference is in spectral selectivity.

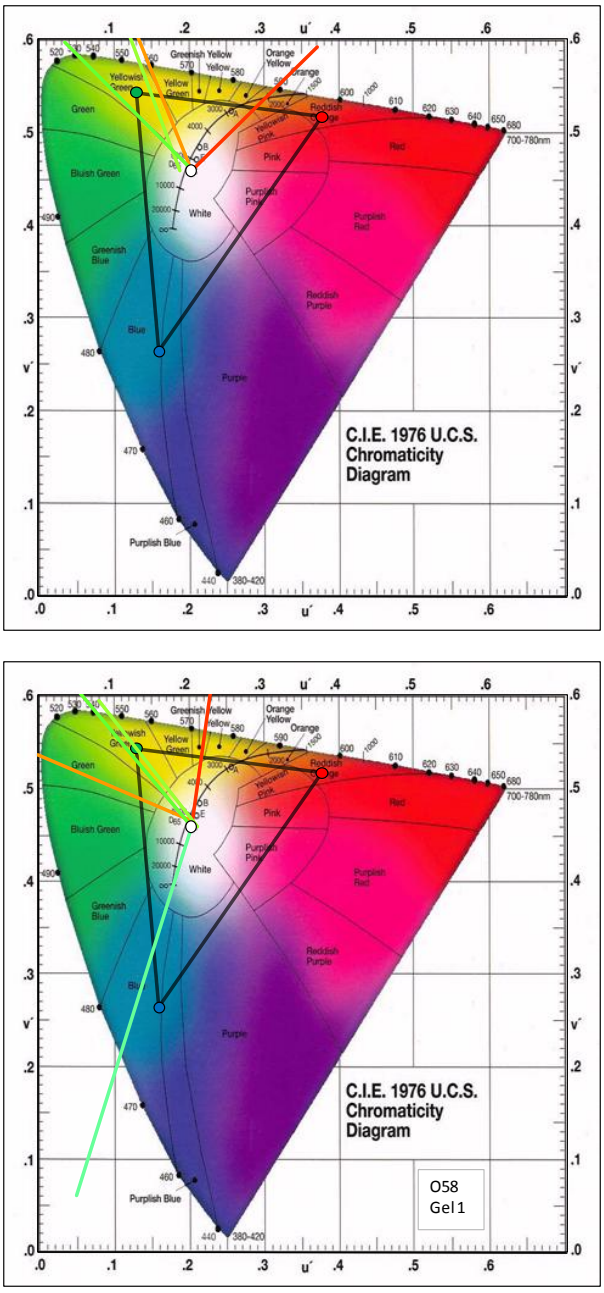

Figure 28 Color appearance zones for Gels 1 and 2 with the ND25 goggle in Experiment 5

The data for the LB145 goggle are shown in Figures 29 and 30. Obviously color naming performance is far superior to performance with the O58 goggle and is not much worse than for the ND25 goggle. The green borders start to shift in Gel 2, the orange borders shift in Gel 5, and borders switch places in Gel 6. By Gel 8, four color zones have been lost: Yellow, Yellow Green, Green, and Purple.

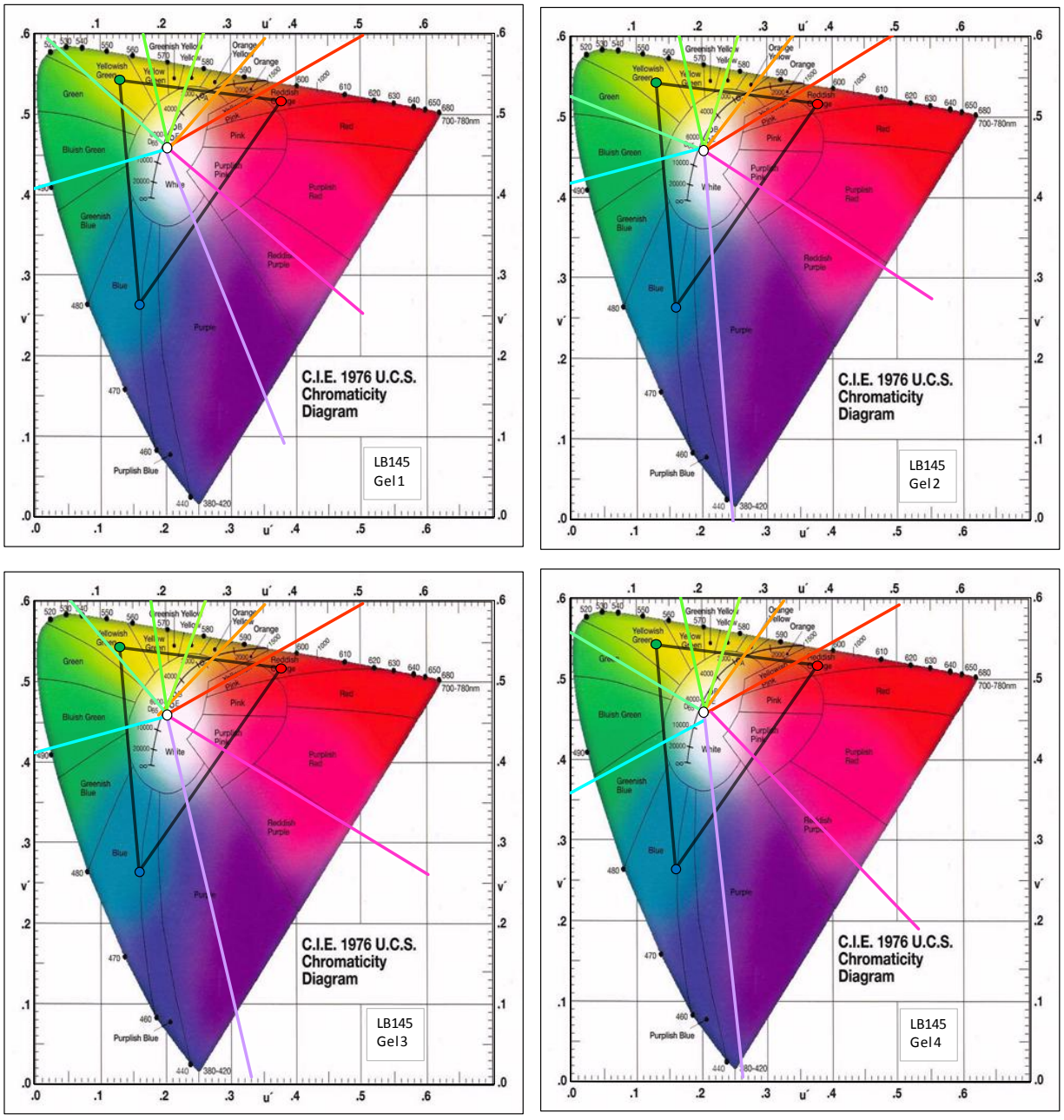

Figure 29 Color appearance zones for Gels 1- 4 with the LB145 goggle in Experiment 5

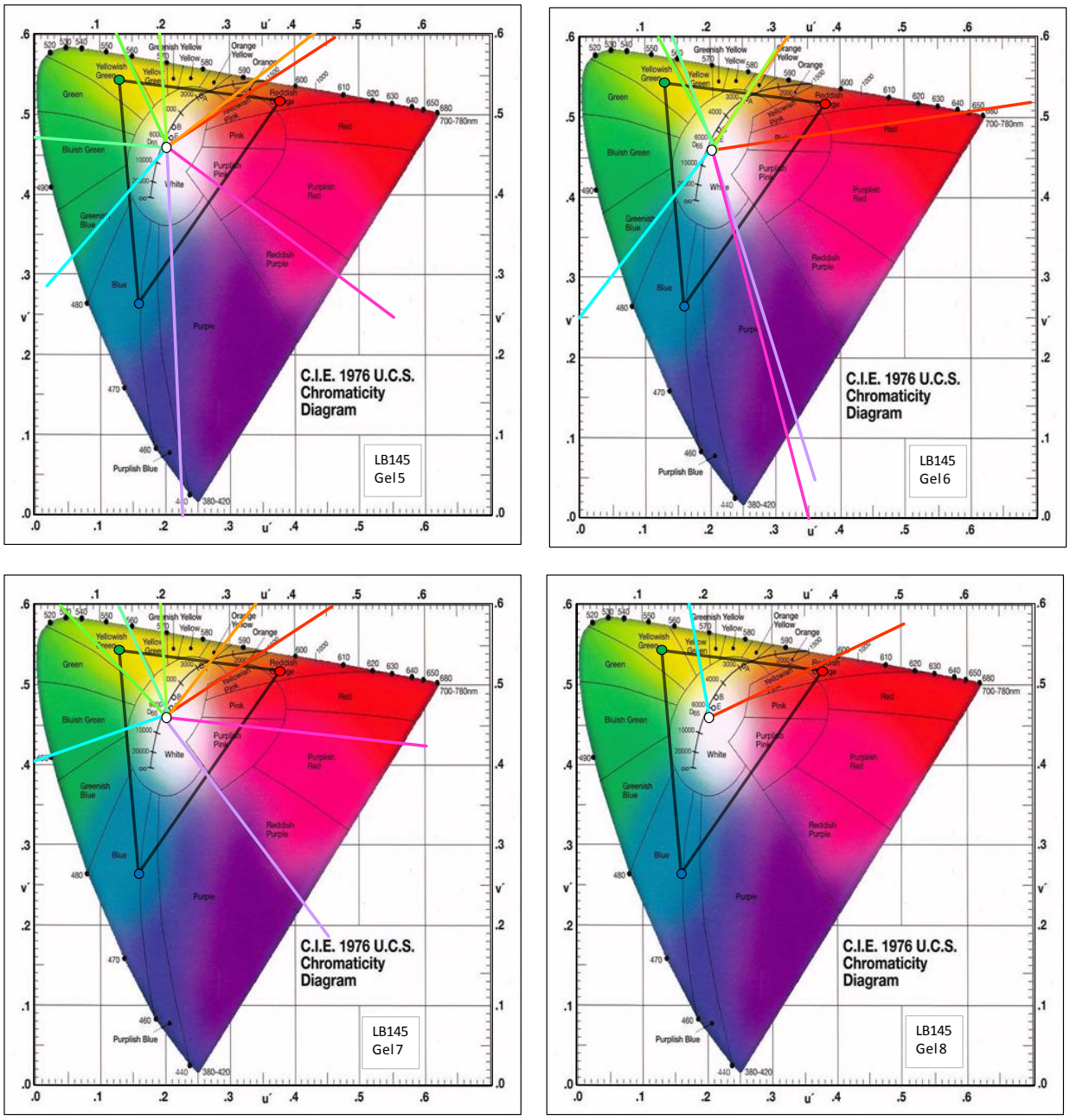

Figure 30 Color appearance zones for Gels 5- 9 with the LB145 goggle in Experiment 5

7.4 Conclusions

These data corroborate the results of Experiment 7, but show the progress across the mesopic range. For the no goggle data, color naming performance remains very good through about 1.1 cd/m² for the median stimulus (remember blue was only 55% of the median luminance). By 0.28 cd/m² for the median stimulus, some borders started to reverse and chromaticity was very poor by 0.07 cd/m² for the median stimulus. Four color zones were totally absent by 0.001 cd/m² for the median stimulus. The data for the ND25 goggle were very similar (when adjusting for the reduced luminance) and the data for the LB145 goggle were not very much worse. On the other hand, color naming with O58 goggle was very poor even for the first gel (about 4.4 cd/m² for the median stimulus). This is consistent with the data from Experiment 7. Remember that the O58 goggle transmits almost all of the power from the red phosphor of the Sony GDM-C520 CRT. It transmits 40% of the power to the l-cone and 20% to the m-cone, but almost no power to the s-cone (0.01%). Clearly s-cone is much more important than the l-cone for color naming in the mesopic range.

8. DISCUSSION

The seven experiments parameterized cone and rod inputs across the mesopic range for brightness, contrast acuity, contrast sensitivity, and color appearance. All of the results were quite consistent with Raphael & MacLeod's (2008) proposed transition from cones to rods at about 0.05 cd/m². Sharpe et al. (2005) have fit the photopic efficiency function with a weight of 0.69 for the l-cone input. While photopic contrast is the best predictor for contrast acuity and contrast sensitivity in the photopic range, these data consistently indicate that l-cone input becomes much less important than m-cone input in the high mesopic range. Noting the warning by Cao, Pokorny, & Smith (2005) that rod input may be interpreted as m-cone input, Experiments 2 & 4 explicitly teased apart the rod and m-cone inputs. In counterpoint to the decline in l-cone contribution, these data consistently reveal the critical importance of s-cone input in the mesopic range. This is especially important for understanding mesopic vision, since s-cone input is not a contributor to the photopic efficiency function. The decline in l-cone input and the importance of s-cone input for luminance, contrast acuity, and contrast sensitivity was mirrored in the color appearance data of Experiments 5 and 7. Color naming performance declined precipitously with the O58 goggles which provided high l-cone transmittance, but almost no s-cone transmittance. The LB145 goggle (which provided high s-cone transmission) produced better color appearance performance than the O58 goggle and was almost as good as the ND25 goggle at maintaining CRT color appearance in the high mesopic range in Experiment 5.

The brightness, contrast acuity, and contrast sensitivity data should inform future models designed to predict aircrew vision in the mesopic range, but the color appearance data can be directly applied to current models used by AFRL/RHDO. For instance LICOM2[28] is used to predict shifts in color appearance due to wearing laser eye protection. It is based on the classic photopic models (Yxy, Lu'v', and Lab). These data can be added to LICOM2 in order to extend its predictions through the mesopic range. These results also suggest that more recent color

appearance models (such as Hunt94, CIECAM97s, or CIECAM02[29]) may improve predictions for aircrew in the mesopic range.

The color zone analysis of Experiment 5 may also inform upgrades to LICOM2. It is not at all clear that the complex set of rules adopted for color naming in Experiments 5 and 7was warranted. While vastly increasing the range of choices available to the participant, it also vastly increased the process of data analysis. Simply limiting chromatic color name responses to the opponent channels (red, yellow, green, and blue) and their intermediate colors (orange, yellow green, blue green, and purple) would have greatly simplified hue angle analysis and produced similar results. Future tasks can use such a restricted set without concern about biasing the results. Instead of relying on the light, dark, and greyish modifiers, the chromaticity contours could be computed from the use of achromatic names (white, grey, and black) and consistency across participants. This again would vastly simplify data analysis while not biasing the results. In short, a simple set of color naming rules and simple analyses in terms of hue angle and chromaticity contours could be used to add a color zone analysis to LICOM2. The color zone analysis in Experiment 5 was more sensitive to the effect of the goggles than the color shift analysis in Experiment 7. Adding color zone analysis in newer color appearance models across the mesopic range could augment the predictive validity of LICOM2.

9. ACKOWLEDGEMENTS

The author is grateful to AFRL 711HPW/ RHDO for the opportunity to perform this research by the award of the HBCU/MI grant and for the support and cooperation of both the UTSA and Wright Patterson IRBs. The research would not have been possible without the invaluable guidance and expertise provided by Leon McLin and Tom Kuyk. The author also thanks Jim Stringham for his help on the heterochromatic flicker photometry tasks and Bill Brockmeier for his help with the Regan letter prototypes, the CIE u'v' templates, and guidance with the OceanOptics spectrophotometer. Finally, the author would like to acknowledge the help of Mary McNair (the Department Administrative Assistant) and the student Research Assistants: Laura Flores, Ryan Giuliano, Daniel Nguyen, and Anissa Snyder.

10. REFERENCES

[1] Hunt, R.W.G. (1994). An improved predictor of colourfulness in a model of colour vision. *Color Research & Application,19,23- 26*.

[2] CIE (1998). *The CIE 1997 Interim Color Appearance Model (Simple Version), CIECAM97s*, CIE Publication 131.

[3] Deng, L., Chen, L., & Rea, M.S. (2005) An evaluation of the Hunt94 color appearance model under different light sources at low photopic to low mesopic light levels. *Color Research and Application, 30, 2, 107- 117*.

[4] Kwak, Y., MacDonald, L.W., & Luo, M.R. (2003). Mesopic colour appearance. *Human Vision and Electronic Imaging, Proceedings of SPIE vol. 5007, 161- 169*.

[5] Shin, J.C., Taguchi, H., & Shiori, A. (2004). Changes of color appearance in photopic, mesopic, and scotopic vision. *Optical Review, 11, 4, 265- 271*.

[6] Cao, D., Pokorny, J., & Smith, V.C. (2005). Matching rod percepts with cone stimuli. *Vision Research, 45, 2119- 2128*.

[7] Eloholma, M . & Halonen, L.(2005). MOVE (Mesopic Optimization of Visual Efficiency): Performance based model for mesopic photometry. Report 35. Helsinki University of Technology, Lighting Laboratory, downloaded 7 FEB 2007 from http://www.lightinglab.fi/CIETC1-58/files/MOVE_Report.pdf.

[8] NHTSA VSR DOT HS 809 884. Downloaded from http://www-nrd.nhtsa.dot.gov/departments/Human%20Factors/810594/pages/3aObjective2.htm

[9] Baldwin, J.B., Dennis, R.J., Ivan, D.J, Miller R.E., Belihar, R.P., Jackson, W.G., Tredici, T.J., Datko, L.M., and Hiers, P.L., (1999). The 1995 Aircrew Operational Vision Survey: Results, Analysis, and Recommendations. *SAM-AF-BR-TR-1999-0003*.

[10] CIE (1926). *Commission Internationale de l'Eclairage Proceedings, 1924*. Cambridge: Cambridge University Press.

[11] CIE Proceedings (1951), Vol. 1, Sec 4; Vol 3, p. 37, Bureau Central de la CIE, Paris, 1951.

[12] Sharpe, L. T., Stockman, A., Jagla, W. & Jägle, H.(2005). A luminous efficiency function, V*(l), for daylight adaptation. Journal of Vision, 5, 948-968.

[13] Kaiser, P. K. (1973). Photopic and mesopic photometry; yesterday, today and tomorrow. In Golden Jubilee of Colour in the CIE. The Society of Dyers and Colourists, Bradford.

[14] http://www.yorku.ca/eye/flicker.htm

[15] Snodderly, D.M., Mares, J.A., Wooten, B.R., Oxton, L., Gruber, M., & Ficek, T. (2004). Macular pigment measurement by heterochromatic flicker photometry in older subjects: The carotenoids and age-related eye disease study. Investigative Ophthalmology & Visual Science, 45 (2), 531-538.

[16] Kaiser, P. K. (1971). "Minimally Distinct Border as a Preferred Psychophysical Criterion in Visual Heterochromatic Photometry," J. Opt. Soc. Am. 61, 966-971

[17] Stockman, A., & Sharpe, L. T. (2000). Spectral sensitivities .of the middle- and long-wavelength sensitive cones derived from measurements in observers of known genotype. *Vision Research*, *40,* 1711-1737.

[18] Raphael, S., & MacLeod, D. I. A. (2008). Minimally distinct borders in mesopic vision [Abstract]. Journal of Vision, 8(17):75, 75a, http://journalofvision.org/8/17/75/, doi:10.1167/8.17.75.

[19] Wandell, B.A. (1995). *Foundations of Vision*. Sinauer Associates; Sunderland, MA.

[20] Rabin, J. (1996). Cone-specific measures of human color vision. *Investigative Ophthalmology & Visual Science, 37, (13), 2771-2774*

.

[21] Cole, G.C. & Hine, T. (1992). Computation of cone contrasts for color vision research. *Behavior Research Methods, Instruments, & Computers, 24 (1), 22-27*.

[22] Ginsburg, A.P. (1984) "A New Contrast Sensitivity: Vision Test Chart," Am. J. Opt. Physiol. Opt., 61(6), 403.

[23] Bailey IL, Lovie JE. New design principles for visual acuity letter charts. Am J Optom Physiol Opt 1976; 53: 740–745.

[24] Widdel, H., & Post, D.L. (1992). *Color in Electronic Displays*. New York: Plenum Press.

[25] Kelly, K.L., & Judd, D.B.(1976). *Color: Universal Language and Dictionary of Names*. U.S. Department of Commerce: Washington D.C.. NBS Special Publication 440.

[26] Berlin, B. & Kay, P. (1969). *Basic Color Terms: Their Universality and Evolution* Univ California Press, Berkeley.

[27] Fairchild, M. D. (2005) *Color Appearance Models (2nd Ed.)*. John Wiley & Sons,; Sussex, England.

[28] Kuyk, T.K.; Irvin, G.E.; & Gaska, J.P. (2001) Air Force laser eye protection lighting compatibility model II.

[29] Moroney, N., Fairchild, M.D., Hunt, R.G.W., Li, C.J., Luo, M.R., & Newman, T. (2002) The CIECAM02 color appearance model, *IS&T / SID Color Imaging Conference, Scottsdale, 23- 27*.